IEEE Access
Multidisciplinary ⋮ Rapid Review ⋮ Open Access Journal

Received April 16, 2021, accepted April 19, 2021, date of publication April 22, 2021, date of current version May 3, 2021.

Digital Object Identifier 10.1109/ACCESS.2021.3074933

Integrated Optimization of Bus Route Adjustment With Passenger Flow Control for Urban Rail Transit

WENLIANG ZHOU[1,2], PANPAN HU[1], YU HUANG[1], AND LIANBO DENG[1,2]
[1]School of Traffic and Transportation Engineering, Central South University, Changsha 410075, China
[2]Rail Data Research and Application Key Laboratory of Hunan Province, Central South University, Changsha 410075, China

Corresponding author: Wenliang Zhou (zwl_0631@csu.edu.cn)

This work was supported in part by the National Natural Science Foundation of China under Grant U1934216, Grant 71871226, and Grant U1834209; in part by the Natural Science Foundation of Hunan Province, China, under Grant 2018JJ3698; and in part by the Fundament Research Funds for the Central Universities of Central South University under Grant CX20200194.

ABSTRACT The contradiction between transport capacity and passenger demand in urban rail transit is usually prominent during peak hours in some megacities of China, and some passenger flow control measures have been adopted to alleviate passenger congestion. To better save passengers' travel time when taking passenger flow control measures, this paper proposes an integrated optimization method of bus route adjustment with network-level passenger flow control for urban rail transit, in which the controlled passengers can freely choose to shift to bus or to retain in urban rail transit for pursuing a lower travel cost. With the objectives of minimizing average additional travel time for all affected passengers and maximizing the operating revenue of urban rail transit, an integer non-linear programming model is formulated to determine the inbound passenger volumes and bus adjustment schemes. To solve this proposed model effectively, a multi-objective particle swarm optimization based on dual-population co-evolution is designed. Finally, three sets of numerical experiments, including an integrated optimization experiment and two independent optimization experiments of passenger flow control, are implemented to demonstrate the feasibility and benefits of the proposed method.

INDEX TERMS Urban rail transit, passenger flow control, bus route adjustment, integrated optimization, dual-population co-evolution.

I. INTRODUCTION

Urban rail transit is a rapid, efficient, punctual and green transportation mode, and plays a significant role in alleviating the traffic pressure. In recent years, it has been in great development, and its scale has been unceasingly expanding, especially in some megacities. With the urban rail transit stepping into network operation, its passenger demand has increased dramatically, but its transport capacity cannot efficiently meet its huge passenger demand, especially during peak hours. In large cities, such as Beijing, Shanghai and Guangzhou, passenger congestion in urban rail stations during peak hours is out of the ordinary serious, which poses a great threat to the operational safety of the urban rail system.

Facing passenger congestion in rail stations, an intuitive solution is to enhance the transport capacity. However, due to the limitation of the maximum transport capacity and the long period for infrastructure construction, enhancing the capacity is a challenging task [1]. As an alternative, implementing some operational measures is a common way. In general, the available measures to release passenger congestion can be classified into two categories. One concentrates on optimizing operation plans, such as train timetables and stops, while the other focuses on passenger demand management, including passenger flow control and fare strategies.

In recent years, some researchers [2]–[5] investigated the service-oriented train timetabling problem under crowded situations to improve the service quality of urban rail transit. Although service-oriented train timetabling indeed shortens the passengers' waiting time, passenger congestion on platforms remains difficult to relieve. A large amount of passengers gathering on the platforms easily brings high risks. Moreover, several researchers tried to study fare strategies to alleviate congestion in rail stations. For example,

The associate editor coordinating the review of this manuscript and approving it for publication was Xinyue Xu.

Wang *et al.* [6] proposed an additional fare strategy to shift a few passengers of a congested station to board/alight at its neighboring uncongested stations. Yang *et al.* [7] put forward a fare-reward scheme to incentivize a shift in departure time to relieve peak-hour congestion at rail stations. These strategies can alleviate passenger congestion to some extent, but it is difficult to determine a reasonable fare strategy in reality.

Passenger flow control (PFC) is a popular measure to alleviate passenger congestion inside rail stations. It makes redundant passengers retain at station halls or outside stations, thus passenger congestion on platforms can be significantly cut down. In practice, some megacities in China have adopted some PFC measures during morning and evening peak hours to ensure the operational safety of rail stations. Specific measures include limiting the passengers' walking speed by setting railings, controlling the inbound passenger volume by closing some gates or ticket machines, and even closing some heavily congested stations. However, these PFC measures are implemented mostly according to operators' subjective experiences, and lack of precise methods [8]. Nowadays, some researchers have noticed this problem and conducted some studies on improving the effectiveness of PFC measures. These studies can be divided into three levels, i.e., station-level, line-level and network-level PFC.

As to station-level PFC, the adopted control measures are usually implemented in various stations respectively, and they are not coordinated among stations. Li and Zhou [9] proposed a dynamic passenger flow analysis algorithm to get refined data of passengers, which can optimize the PFC strategy in a transfer station. Xu *et al.* [10] developed a queuing analytical model to calculate the station service capacity and guide the PFC for a single station during peak hours. Xu *et al.* [8] focused on the PFC inside a station under uncertain demand and proposed a detailed procedure of PFC under various demand scenarios. Moreover, Zhang *et al.* [11], Baee *et al.* [12] and Seriani *et al.* [13] devoted to simulating passengers' boarding and alighting behavior to optimize the PFC strategy inside a station.

Since station-level PFC is prone to neglect the impact of inbound passengers at upstream stations to that in downstream stations, its effect of relieving congestion is relatively limited on a rail line with multiple crowded stations. Hence, plenty of researchers [1], [14]–[19] turned to line-level PFC, which synergistically imposes PFC measures at multiple rail stations. For example, Wang *et al.* [14] studied the joint PFC problem between stations on a rail line to minimize the average passenger delay. By considering the dynamic propagation features of passenger flow, Jiang *et al.* [15] developed a dynamic PFC model on a metro line for maximizing the comprehensive profit of both boarding passengers and limited passengers. Shi *et al.* [17] proposed a method for collaboratively optimizing the origin-destination PFC strategies of multiple stations. Jiang *et al.* [1] designed an optimization scheme to solve the coordinated control problem of passenger inflow for a rail line. Furthermore, Jiang *et al.* [18] combined skip-stopping and PFC on a single line, and put forward a novel Q-learning approach to solve the combined optimization problem.

Compared with station-level PFC, line-level PFC has achieved great progress in alleviating congestion among multiple stations, but it overlooks the interactions between several lines at transfer stations. Thus, it is hard for line-level PFC to relieve congestion of transfer stations [20]. With the network operation of urban rail transit, many transfer stations are under great pressure as the increase of transfer passengers. Therefore, network-level PFC is urgently needed, and through taking coordinated PFC measures to multiple stations in the network simultaneously, the congestion in the whole network can be better alleviated. Up to now, several researchers have concerned on this problem. For instances, Zeng *et al.* [21], Kong and Zhang [22] developed some methods from the view of network controllability, to identify critical stations for carrying out PFC on an urban rail network. Xu *et al.* [20] formulated a bi-level programming model to address the PFC problem in a metro network, and tried to simultaneously control the inbound and transfer passengers at transfer stations. Shi *et al.* [23] derived a cooperative PFC method for a metro network by considering the dynamic characteristics and transfer behaviors of passengers.

Network-level PFC can effectively reduce passenger accumulation on platforms, nevertheless, it inevitably causes some passengers to lose the access to travel in time as they are prohibited from entering the station instantly. Since a majority of passengers during peak hours are for commuting purposes and willing to wait at station halls, plenty of waiting passengers and long waiting time are prone to riots. To save passengers' waiting time, the evacuation of controlled passengers is as important as PFC. Generally, bus bridging is recognized as an excellent way to evacuate passengers under such circumstances, and some researchers have researched the problem of bus bridging service design for crowded commuting urban rail lines or under the disruption of an urban rail system. To mitigate overcrowded situation for commuting metro lines, Yang *et al.* [24] proposed a two-stage mathematical model, firstly determined the stations and periods for taking PFC strategy in stage 1, and specially exploited inter-line and parallel bus-bridging services to transport these commuters affected by PFC in stage 2. Incorporating the uncertainty of bus travel time, Liang *et al.* [25] developed a robust approach to bus bridging service design under the disruption of an urban rail system. Jin *et al.* [26] proposed a measure of enhancing the capacity of bus services, so as to improve the connectivity of an integrated metro-bus network and enhance the resilience of a metro network. Jin *et al.* [27] presented a bus bridging service design approach to respond the disruption of an urban rail network. For providing bus-bridging services, most researches considered organizing new bus routes, which will result in high costs. This paper considers to service the controlled passengers by adjusting some existing bus routes to stop at these bus stations near the controlled rail stations. In this way, the controlled passengers can expediently shift to the bus system with a relatively low cost.

In summary, the combination of bus route adjustment (BRA) with PFC of urban rail cannot only effectively reduce the accumulation of passengers and ensure the safe operation of rail stations, but also enhance the travel efficiency of controlled passengers.

This paper devotes to integrating BRA with network-level PFC of urban rail transit during peak hours, and aims to achieve their integrated optimization. Network-level PFC is adopted to alleviate the operational pressure in a crowded urban rail network, while BRA, as a supplementary measure, is to minimize the negative effect of PFC. Compared with the existing research, we try to provide the following contributions.

(1) BRA strategy is first integrated with the urban rail network-level PFC problem. The combination of BRA with PFC cannot only effectively strengthen the operational safety at rail stations, but also quickly evacuate some controlled passengers with relatively short travel time.

(2) An integrated optimizing model of BRA with PFC for urban rail transit is formulated to minimize the average additional travel time of all affected passengers based on the effective utilization of train capacity.

(3) A multi-objective particle swarm optimization based on dual-population co-evolution (DPCMOPSO) is designed to solve the proposed model. It introduces a hybrid constraint processing method of feasible and infeasible population concurrent evolution, as well as infeasible solutions repair, and this method can better ensure the convergence speed and improve the global search ability of the algorithm.

The rest of this paper is organized as follows. In Section II, we describe the integrated optimization problem of BRA with urban rail PFC in detail. In Section III, the choices of shift and retention behavior for controlled passengers are analyzed. In Section IV, the additional travel time of shifted passengers, retained passengers and original bus passengers are analyzed respectively. In Section V, the studied problem is formulated as an integer non-linear programming model. In Section VI, a multi-objective particle swarm optimization based on dual-population co-evolution (DPCMOPSO) is proposed to solve the model. In Section VII, numerical and comparative experiments are conducted, and Section VIII summarizes this research and discusses further studies.

II. PROBLEM DESCRIPTION

This section firstly details the direction-based PFC problem in the urban rail network and its corresponding BRA problem. Then the integrated optimization problem of BRA with network-level PFC is described.

A. DIRECTION-BASED PFC IN URBAN RAIL NETWORK

Passenger flow control (PFC) of urban rail transit is to control the inbound or transfer passengers by utilizing the gates, escalators and other facilities. When the remaining capacity of arriving trains is far from meeting passenger demand, operators needs to take PFC measures, which can avoid accident risks caused by passenger accumulation on platforms, such as trampling, falling into the track. PFC can not only relieve passenger congestion inside rail stations but also guarantee the travel safety for passengers. According to the refinement degree of PFC at rail stations, there are usually the following three types of PFC.

(1) Total-volume-based PFC, which aims to control the total volume of inbound passengers without distinguishing their directions and destinations.

(2) Direction-based PFC, which is to carry out PFC for the up and down directions at a station, respectively.

(3) Origin-destination-based PFC, which is to control the inbound passenger volume separately for each destination.

As shown in Fig. 1, a bidirectional rail line contains A, B, C, D and E five stations, in which station C is a PFC station. Three types of PFC are illustrated in Fig. 1(a), Fig. 1(b) and Fig. 1(c), respectively.

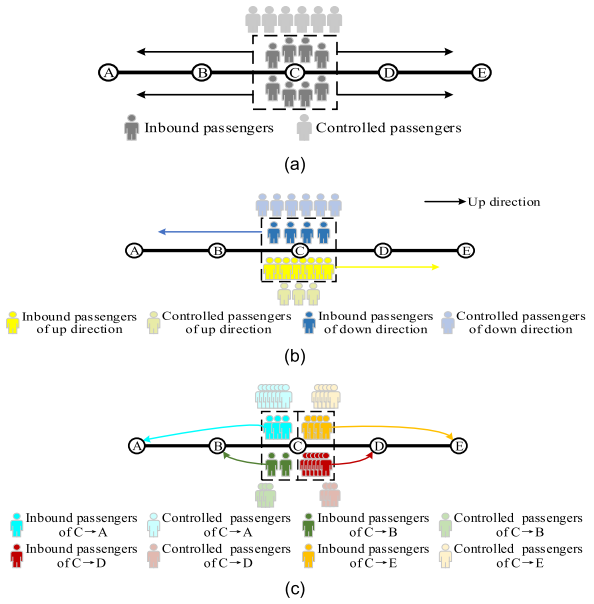

FIGURE 1. Illustration of three types of PFC. (a) Total-volume-based PFC. (b) Direction-based PFC. (c) Origin-destination-based PFC.

At each rail station, the numbers of arriving passengers in the up and down directions are often unbalanced, and the remaining capacities of approaching trains from two directions are also unbalanced. Total-volume-based PFC is inclined to cause capacity waste in the direction with fewer passengers but large remaining capacity. Origin-destination-based PFC can achieve accurate control and ensure the effective utilization of train capacity in theory. However, it is hard to implement in practice because of the large number of passengers' terminal stations. As a synthesis of the above two ways, direction-based PFC takes both advantages into account, and it cannot only make better use of the capacity but also be conducted potentially after making some adjustments to station facilities and organization methods.

To alleviate the congestion of multiple stations in an urban rail network, a coordinated PFC is necessary [28]. This paper focuses on the multi-station direction-based coordinated PFC

in an urban rail network, in which passenger congestion arises in lots of stations during peak hours. It is committed to optimizing an appropriate inbound passenger volume for each station in the up and down directions by considering the interrelationship among stations. The ultimate goal is to reduce the travel time of passengers caused by PFC on the premise of safe operation. Assume that the studied urban rail network consists of a set of stations and a set of sections, denoted by S and D, respectively. The set of PFC stations is denoted by $\tilde{S}$, $\tilde{S} \in S$. Each transfer station is distinguished as two or more different stations according to the number of its connected lines; each transfer channel is regarded as a transfer section. As the arriving passenger volume of a station varies with time, we discretize peak hours into several PFC periods of equal length, and denote the set of PFC periods as T.

B. BRA FOR PFC OF URBAN RAIL TRANSIT

PFC of urban rail transit plays an important role in avoiding passenger congestion inside rail stations during peak hours, nevertheless, it also brings the problem that some passengers are unable to enter the station and travel in time. During peak hours, most passengers are commuters, they tend not to give up their travel or adjust travel time even though they are controlled in origin stations. Controlled passengers usually have two choices, one is to retain in station halls until they are permitted to enter platforms for boarding trains, and the other is to shift and travel by bus promptly. The first choice will not only lead to a prolonged waiting time but also cause numerous passengers to gather in station halls, which may seriously threaten the operational order and safety of the urban rail system. Thus, it is better to induce more passengers to shift to the bus system. To provide more convenient bus travel for controlled passengers, some existing bus routes can be selected and adjusted to pass through the adjacent bus stations of the PFC stations. Once adjusted, controlled passengers can expediently take this adjusted bus route to shift to the bus system to finish their travel.

For each PFC station, we can pick out some existing bus routes as its candidate adjustable bus routes in advance, and determine the corresponding bus adjustment schemes based on four principles, which are listed below.

(1) To facilitate the scheduling and management of bus depots, the origin and terminal stations of each bus route should be consistent before and after the BRA.

(2) To weaken the impact on original bus passengers, the orientation and stopping stations of each bus adjustment scheme should overlap with the original route as much as possible.

(3) To effectively serve the shifting passengers from the urban rail system, the candidate adjustable bus routes should have a certain surplus capacity.

(4) To ensure that the adjusted bus routes could attract controlled passengers, the bus adjustment schemes must pass through the bus stations near two or more PFC stations, and the distance between rail stations and bus stations should be as short as possible.

We define L_r as the set of candidate adjustable bus routes for PFC station $r \in \tilde{S}$. For any candidate adjustable bus route $l \in L_r$, it does not pass through any bus station near PFC station r before adjustment, however, it will pass through a nearby bus station of station r once adjusted. The bus adjustment schemes of bus route l for PFC station r, denoted by $\bar{l}_r$, must stop at least one bus station near station r. Note that for different PFC stations, a particular existing bus route corresponds to various bus adjustment schemes.

With the set of candidate adjustable bus routes L_r for PFC station $r \in \tilde{S}$ and the pre-determined adjustment scheme $\bar{l}_r$ of bus route $l \in L_r$, the problem of bus route adjustment (BRA) for PFC is defined as selecting some candidate adjustable bus routes to adjust, so as to provide outstanding services for controlled passengers in PFC stations. We define a binary variable Y_l^r to indicate whether the candidate adjustable bus route $l \in L_r$ for station r is selected to adjust, if selected, $Y_l^r = 1$, indicating that bus route l will be adjusted to bus route $\bar{l}_r$; otherwise, $Y_l^r = 0$, and bus route l remains unchanged.

To better explain the problem of BRA for PFC, a simple example is shown in Fig. 2. An urban rail line contains 7 stations, of which stations B and D are identified as PFC stations. Bus routes 1 and 3 are candidate adjustable bus routes for PFC station D, and bus routes 2 and 4 serve as candidate adjustable bus routes for PFC station B. If bus routes 1 and 3 are confirmed to adjust for station D, they will be adjusted to bus routes 5 and 6, passing through bus stations u and w severally. Similarly, to evacuate the controlled passengers in station B, bus routes 2 and 4 can be adjusted to bus routes 7 and 8, both passing through bus station q. Moreover, it is also viable to adjust bus route 1 to bus route 9, stopping at bus station p, and serve station B.

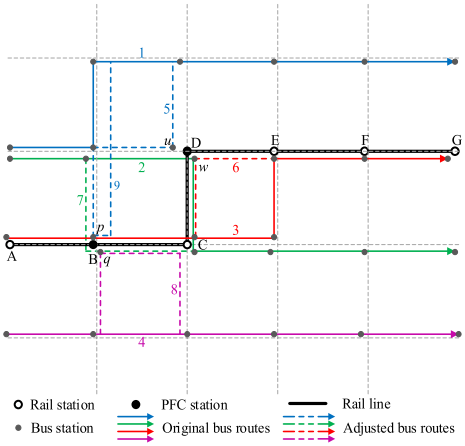

FIGURE 2. A simple example of BRA for PFC of urban rail transit.

C. INTEGRATED OPTIMIZATION OF BRA WITH PFC

The PFC strategy of urban rail transit determines the number of controlled passengers at rail stations, and the BRA strategy makes some controlled passengers attracted by the

TABLE 1. Symbols and definitions of the input parameters.

Objects	Symbols	Definitions
PFC periods	T	Set of PFC periods
	$\|T\|$	Number of PFC periods
	$\Delta\tau$	The length of a PFC period
	τ	Index of PFC period, $\tau = 1,2,3,\cdots,\|T\|, \tau \in T$
Urban rail network	S	Set of urban rail stations
	r, s, k	Index of urban rail station, $r, s, k \in S$
	$\tilde{S}$	Set of PFC stations
	D	Set of sections in the urban rail network, includes rail sections and transfer channels
	d	Index of section, $d \in D$
	$\overline{D}$	Set of rail sections
	$D \backslash D$	Set of transfer channels
	F	Set of urban rail directions, includes up and down directions.
	f	Index of urban rail direction, $f = 1$ represents up direction, $f = 2$ indicates down direction, $f \in F$
	G_r	Passing capacity of all entry gates in rail station r during a PFC period
	$R_d(\tau)$	Transport capacity of rail section d during PFC period τ
	UTC_d	Passing capacity of unidirectional transfer channel d during a PFC period
	$BTC_{d-d'}$	Passing capacity of bidirectional transfer channel $d - d'$ during a PFC period
	$h_r^f(\tau)$	The number of trains arriving at direction f of rail station r during PFC period τ
	P_r	Platform capacity in rail station r
Passenger flow	$P_{rs}(\tau)$	Newly arriving passenger volume of OD (r, s) during PFC period τ
	$P_r^f(\tau)$	Newly arriving passenger volume of direction f at rail station r during PFC period τ
	$Q_{rd}^f(\tau^0, \tau)$	The probability that a passenger departing from direction f of rail station r during period τ^0 pass through the section d at PFC period τ ($\tau^0 \leq \tau$)
Bus network	V	Set of bus stations
	v, w	Index of bus station, $v, w \in V$
	L_r	Set of candidate adjustable bus routes for PFC station $r \in \tilde{S}$
	l	Index of candidate adjustable bus route, $l \in L_r$
	$\bar{l}_r$	A bus adjustment scheme obtained by adjusting l to a bus station near rail station r
	n_{max}	The maximum number of bus routes allowed to be adjusted in bus network
	m_v^0	Number of bus routes stopping at bus station v before adjusting bus routes
	m_v^{max}	The maximum number of bus routes allowed to stop at bus station v

bus system. The BRA strategy directly affects the retained passenger volumes of the subsequent PFC periods, which affects the PFC strategy in the urban rail network in reverse. Hence, the problems of optimizing PFC and BRA strategies are mutually interdependent. This paper is devoted to the integrated optimization of BRA with PFC for urban rail transit, aiming to shorten travel time for passengers while relieving the passenger congestion of urban rail transit during peak hours.

To simplify the integrated optimization problem, we make the following assumptions throughout this paper.

(1) The urban rail passengers can quickly leave platforms after getting off trains, and their occupation of platforms is negligible.

(2) The bus schedule is known and fixed, and the departure interval is consistent before and after the BRA.

(3) The urban rail passengers abandoning travel is not considered, and the retained passengers will not change their travel paths. The unaffected bus passengers of BRA will insist on their original bus paths, while the affected bus passengers will still travel by bus instead of shifting to the urban rail system.

The input parameters of this research mainly include four parts, i.e., PFC period parameters, urban rail network parameters, passenger flow parameters and bus network parameters. Their symbols and definitions are listed in Table 1.

The PFC strategy of urban rail transit needs to optimize the permitted inbound passenger volume for each PFC period. To avoid repeated adjustments of bus routes, the BRA strategy only needs to decide whether to implement the bus adjustment schemes throughout peak hours, rather than for each PFC period. In brief, if a bus route is selected to be adjusted, the whole peak hours will apply the adjusted route. The detailed decision variables are listed in Table 2.

III. THE BUS-SHIFT OR RETENTION CHOICES OF CONTROLLED PASSENGERS

Due to the implementation of PFC measures at rail stations, some passengers are controlled and not permitted to enter platforms during their arrival periods. The controlled passengers can choose to wait in the urban rail system or to shift to the bus system. This section will explain in detail how to determine the number of controlled passengers shifting to the bus system and retaining in the urban rail system.

The controlled passenger volume is the difference between the demand volume and the permitted inbound passenger volume. In the first PFC period, the demand volume of inbound

TABLE 2. Symbols and definitions of the decision variables.

Types	Symbols	Definitions
PFC decision variables	$X_r^f(\tau)$	Integer decision variable, the permitted inbound passenger volume in direction f of rail station r during PFC period τ
BRA decision variables	Y_l^r	Binary decision variable, adjustment indicator of bus route l to bus route $\bar{l}_r$ for PFC station r, if bus route l is adjusted to bus route $\bar{l}_r$, $Y_l^r = 1$; otherwise, $Y_l^r = 0$

passengers is the newly arriving passenger volume, and in the subsequent periods, it includes the newly arriving passenger volume and the retained passenger volume of the previous periods. Hence, the controlled passenger volume in direction f of PFC station r during period τ, denoted by $C_r^f(\tau)$, can be described as Eq. (1).

$$C_r^f(\tau) = \begin{cases} P_r^f(\tau) - X_r^f(\tau) & \tau = 1 \\ P_r^f(\tau) + S_r^f(\tau - 1) & \\ -X_r^f(\tau) & \tau = 2, 3, \cdots, |T| \end{cases}, \quad \forall r \in \tilde{S}, \forall f \in F \quad (1)$$

where $S_r^f(\tau - 1)$ is the retained passenger volume in direction f of station r during period $(\tau - 1)$. As we do not consider the passenger retention before peak hours, i.e., $S_r^f(0) = 0$, the Eq. (1) can be simplified as Eq. (2).

$$C_r^f(\tau) = P_r^f(\tau) + S_r^f(\tau - 1) - X_r^f(\tau), \quad \forall \tau \in T, \ \forall r \in \tilde{S}, \forall f \in F \quad (2)$$

PFC rate is define as the ratio of the controlled passengers to the total inbound passenger demand volume. Thus the PFC rate of direction f at station r during period τ, denoted by $\mu_r^f(\tau)$, can be calculated as Eq. (3).

$$\mu_r^f(\tau) = \frac{C_r^f(\tau)}{P_r^f(\tau) + S_r^f(\tau - 1)}, \ \forall \tau \in T, \ \forall r \in \tilde{S}, \forall f \in F \quad (3)$$

This paper takes a direction-based PFC at each rail station, without distinguishing passengers' destinations in the same direction, the PFC rate of different terminals in a direction can be simplified as the same. Combining the PFC rate with the demand volume of inbound passengers between an origin station and a destination station (hereinafter abbreviated as OD), the controlled passenger volume of this OD can be obtained. Thus, the controlled passenger volume of OD (r, s) during period τ, denoted by $C_{rs}(\tau)$, can be characterized as Eq. (4).

$$C_{rs}(\tau) = \mu_r^f(\tau) \times [P_{rs}(\tau) + S_{rs}(\tau - 1)], \quad \forall \tau \in T, \forall r \in \tilde{S}, \forall s \in \mathrm{S}, \forall (r, s) \in f \quad (4)$$

where $(r, s) \in f$ indicates that passengers of OD (r, s) choose the trains of direction f to travel.

The controlled passengers of each OD face two options of retaining to travel by urban rail transit or shifting to travel by bus. Generally, passengers' travel choice depends on many factors, of which travel time and travel fare are two main ones [29]. Thus we consider these two factors to form two generalized costs for retaining and shifting, respectively, and adopt them to determine the retained and shifted passenger volume.

A. THE GENERALIZED COST FOR RETAINING IN THE URBAN RAIL SYSTEM

When the controlled passengers choose to retain in the station halls, and wait to travel by trains, they have to bear not only the in-vehicle travel time and fare but also the additional waiting time at the station halls (also known as the retention time). Compared with the newly arriving passengers, retained passengers have priority in entering the platforms, so the retention time mainly depends on the number of retained passengers and the available capacity of arrival trains. Thus, the average retention time of the retained passengers in direction f of PFC station r during period τ, denoted by $t_{re}^{r,f}(\tau)$, can be calculated as Eq. (5).

$$t_{re}^{r,f}(\tau) = \frac{S_r^f(\tau - 1)}{CAP_r^f(\tau)} \times \Delta\tau, \ \forall \tau \in T, \ \forall r \in \tilde{S}, \ \forall f \in \mathrm{F} \quad (5)$$

where $CAP_r^f(\tau)$ is the total available capacity of arrival trains in direction f of rail station r during PFC period τ. On this basis, the generalized travel cost for the controlled passengers of OD (r, s) choosing retention during period τ, denoted by $c_{rs}^{urt}(\tau)$, can be characterized as Eq. (6).

$$c_{rs}^{urt}(\tau) = \lambda \times \left(\check{t}_{rs}^{urt}(\tau) + t_{re}^{r,f}(\tau)\right) + m_{rs}^{urt}, \quad \forall \tau \in T, \forall r \in \tilde{S}, \forall s \in \mathrm{S}, \forall f \in F \quad (6)$$

where $\check{t}_{rs}^{urt}(\tau)$ is the travel time of OD (r, s) by urban rail transit during period τ when passengers can directly enter the platform without waiting, m_{rs}^{urt} is the urban rail transit fare for OD (r, s), and λ is the unit time cost.

B. THE GENERALIZED COST FOR SHIFTING TO THE BUS SYSTEM

When the controlled passengers choose to shift and travel by bus, the generalized travel cost also includes travel time and bus fare, in which travel time consists of the walking time from PFC stations to bus stations, bus waiting time, in-bus time, transfer time and walking time from bus stations to destinations. There are many feasible bus paths for controlled passengers. As this paper only takes BRA once for the whole peak hours, the feasible shifting path are same throughout the peak hours.

To determine the feasible shifting paths for controlled passengers, a travel network for shifted passengers is constructed

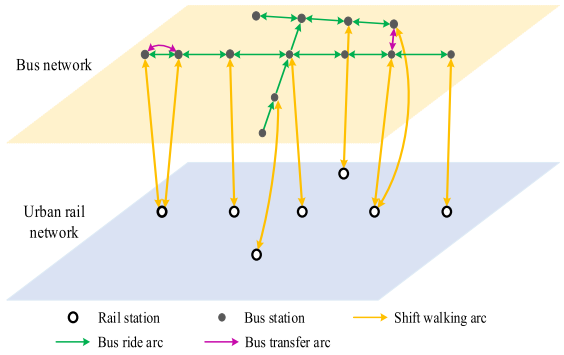

FIGURE 3. Travel network for shifted passengers.

as Fig. 3. When the walking time between a PFC station and a bus station is less than a certain threshold, the two are connected by a shift walking arc. Bus stations can be connected by bus ride arcs and bus transfer arcs. When there are bus routes passing and stopping between two bus stations, the two stations are connected by a bus ride arc. When the walking time between two bus stations is less than a certain threshold, they are connected by a bus transfer arc. Controlled passengers could shift to the bus network through shift walking arcs, then travel by bus ride arcs and bus transfer arcs in the bus network, and finally reach their destination via shift walking arcs.

In the travel network for shifted passengers, we first adopt a depth first search algorithm (DFS) to search for all feasible shifting paths for passengers of each urban rail OD. Obviously, these paths only include walking time from rail stations to bus stations, in-bus time, transfer time and walking time, while bus waiting time and bus fares are not included. To determine the bus waiting time and fare of a path, we should search for its available bus routes. Through the above two steps, we can obtain the travel time and bus fare of all feasible shifting paths. We use I_{rs} to denote the set of feasible shifting path of OD (r, s), $i \in I_{rs}$, $t_{rs}^{bus,i}$ and $c_{rs}^{bus,i}$ to denote the travel time and generalized travel cost for path i of OD (r, s), and they can be characterized as follows.

$$t_{rs}^{bus,i} = t_{rs,walk}^{bus,i} + t_{rs,on}^{bus,i} + t_{rs,wait}^{bus,i}, \quad \forall \tau \in T, \forall r \in \tilde{S}, \forall s \in \mathrm{S}, \forall i \in I_{rs} \tag{7}$$

$$c_{rs}^{bus,i} = \lambda \times t_{rs}^{bus,i} + m_{rs}^{bus,i}, \forall \tau \in T, \forall r \in \tilde{S}, \quad \forall s \in \mathrm{S}, \forall i \in I_{rs} \tag{8}$$

where $t_{rs,walk}^{bus,i}$, $t_{rs,in}^{bus,i}$ and $t_{rs,wait}^{bus,i}$ are the walking time, in-bus time and waiting time for path i of OD (r, s), respectively, in which the walking time includes the shift walking time and the transfer walking time, $m_{rs}^{bus,i}$ is the bus fare by path i.

Only when the generalized cost for a shifting path is less than that of retention, will the controlled passengers choose this path to shift, and this path is called an effective shifting path. By comparing the generalized cost of retention with that of all feasible shifting paths, the set of effective shifting paths of an OD during a PFC period can be obtained. After that, the passenger flow assignment is conducted for the controlled passengers to determine their shifted and retained volumes.

Obviously, controlled passengers prefer to choose the shifting paths with the lowest cost. However, since the original bus passengers have occupied some capacity, the residual capacity of each shifting path is limited. Hence, we take the residual capacity of each effective shifting path into account, and assign the controlled passengers into effective shifting paths according to ascending order of generalized cost. Specifically, we first assign the controlled passengers to the shortest effective shifting path until its capacity is fully used, then assign the controlled passengers to the second shortest effective shifting path under the capacity limit, and so on. Only when all controlled passengers are assigned to the bus network or there is no effective shifting path with residual capacity, will we terminate the passenger flow assignment. The controlled passengers assigned to the effective shifting paths are shifted passengers, and the other passengers are retained passengers.

We use J_{rs}^{t} to denote the set of effective shifting path of OD (r, s) during PFC period τ, $j \in J_{rs}^{\tau}$; $T_{rs}^{j}(\tau)$ to denote the number of shifted passengers assigned to path j. The shifted and retained passenger volumes of OD (r, s) during PFC period τ, denoted by $T_{rs}(\tau)$ and $S_{rs}(\tau)$ respectively, can be calculated as Eq. (9) and Eq. (10).

$$T_{rs}(\tau) = \sum_{j \in J_{rs}^{\tau}} T_{rs}^{j}(\tau) \tag{9}$$

$$S_{rs}(\tau) = C_{rs}(\tau) - T_{rs}(\tau) \tag{10}$$

The shifted and retained passenger volumes for direction f of PFC station r during period τ, denoted by $T_r^f(\tau)$ and $S_r^f(\tau)$ respectively, can be calculated as Eq. (11) and (12).

$$T_r^f(\tau) = \sum_{s \in S, (r,s) \in f} T_{rs}(\tau), \quad \forall \tau \in T, \forall r \in \tilde{S}, \forall f \in F \tag{11}$$

$$S_r^f(\tau) = \sum_{s \in S, (r,s) \in f} S_{rs}(\tau), \quad \forall \tau \in T, \forall r \in \tilde{S}, \forall f \in F \tag{12}$$

IV. ADDITIONAL TRAVEL TIME FOR PASSENGERS

For controlled passengers, they may take some additional travel time, such as waiting time when choosing to retain and walking time when shifting to the bus system. Furthermore, the BRA strategy will affect the original bus passengers and extend their travel time. For better evaluating the influence of obtained PFC and BRA strategies on passengers, this section will analyze the additional travel time for the retained passengers, shifted passengers and original bus passengers, respectively.

The additional travel time for retained passengers is reflected as an extra retention time at station halls. Thus the total additional travel time for all retained passengers, denoted by T_s^{add}, can be calculated as Eq. (13).

$$T_s^{add} = \sum_{\tau \in T} \sum_{r \in \tilde{S}} \sum_{f \in F} \left(S_r^f(\tau) \times t_{re}^{r,f}(\tau) \right) \tag{13}$$

As for shifted passengers, they originally expect to travel by urban rail transit, however, PFC measures are taken in their origin stations, and they must wait for a long time before entering the platforms. As a consequence, they chose to shift to the bus system instead of traveling by urban rail transit. Hence, their additional travel time can be expressed as the difference between the actual bus travel time and the expected urban rail travel time.

The actual bus travel time for shifted passengers is the travel time on their shifting paths. The total actual bus travel time for all shifted passengers, denoted by T_t', can be calculated as Eq. (14).

$$T_t' = \sum_{\tau \in T} \sum_{r \in \tilde{S}} \sum_{s \in S} \sum_{j \in J_{rs}^{\tau}} \left(T_{rs}^{j}(\tau) \times t_{rs}^{bus,j} \right) \tag{14}$$

The expected time is the travel time with sufficient urban rail capacity and without PFC measures. $\check{t}_{rs}^{urt}(\tau)$, mentioned in Section III, is the expected travel time of OD (r, s) during period τ. The expected urban rail travel time for all shifted passengers, denoted by T_t^0, can be calculated as Eq. (15).

$$T_t^0 = \sum_{\tau \in T} \sum_{r \in \tilde{S}} \sum_{s \in S} \left(T_{rs}(\tau) \times \check{t}_{rs}^{urt}(\tau) \right) \tag{15}$$

As a summary, the total additional travel time for all shifted passengers, denoted by T_t^{add}, can be calculated as Eq. (16).

$$T_t^{add} = T_t' - T_t^0 \tag{16}$$

The BRA strategy for PFC will bring inconveniences to some original bus passengers while facilitating the travel of controlled passengers. The BRA strategy tends to detour to these bus stations near the PFC stations, and may cross some bus stations, which causes some original bus passengers to extend their travel time or fail to reach their destinations. Fig. 4 explains the passengers affected by the BRA strategy. For PFC station B, bus routes 1 and 4 have an adjustment scheme severally, which are bus routes 5 and 8 respectively. The crossed segments of route 1 and route 4 are (u, v) and (w, z), respectively, excluding endpoints u, v, w and z. For the passengers on bus route 1, if their origin stations stand before crossed segment (u, v) and destination stations stand after crossed segment (u, v), i.e., passengers from station a or b to station d, e, f or g, their travel time will increase significantly; if their origin or destination stations are located on crossed segment (u, v), i.e., station c, passengers will be unable to travel by their original routes. Similarly, when bus route 4 is adjusted to bus route 8, the travel time of these passengers whose origin stations are h or i and destination stations are j, k, m or n will be remarkably enhanced. Since there is no bus station on crossed segment (w, z), adjusting bus route 4 to bus route 8 will not result in passengers being incapable of traveling. In summary, if a bus route is adjusted, these passengers whose origin stations stand before or on the crossed segment and destination stations stand after or on the crossed segment will be affected.

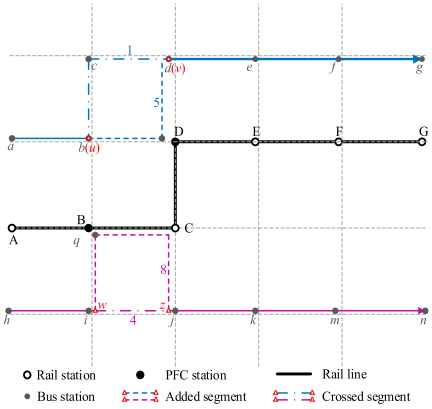

FIGURE 4. Explanatory of the passengers affected by the BRA strategy.

With a given BRA strategy, we can obtain the adjusted bus network and find out the affected bus OD during peak hours, whose affected passenger volume can also be counted. According to assumption (3), the affected bus passengers will reselect their travel paths in the adjusted bus network. DFS algorithm is also adopted here to search for feasible paths for the affected bus passengers of each bus OD, and the passenger flow assignment is carried out in ascending order of generalized cost. It is worth noting that the affected bus passengers are prior to the controlled passengers, i.e., the affected passengers should be assigned before the shifting of controlled passengers is taken into account. If there are remaining affected passengers unassigned when the passenger flow assignment is terminated, the travel time of these passengers is set to a big value.

We use $P(v, w)$ to denote the affected passenger volume of OD (v, w), $\hat{t}(v, w)$ and $\bar{t}(v, w)$ to denote the average travel time for affected passengers of OD (v, w) before and after the BRA, respectively. Hence, the additional travel time for original bus passengers, denoted by T_b^{add}, can be calculated as Eq. (17).

$$T_b^{add} = \sum_{(v,w)} \left[P(v, w) \times \left(\bar{t}(v, w) - \hat{t}(v, w) \right) \right] \tag{17}$$

V. MATHEMATICAL MODELING

This section first defines a spatio-temporal propagation coefficient of passenger flow in urban rail transit, which can be applied to determine the passenger throughput of sections. After that, an integrated optimization model of BRA with PFC for urban rail transit is formulated, with the objective functions and constraints are introduced.

A. THE SPATIO-TEMPORAL PROPAGATION COEFFCIENT OF URBAN RAIL TRANSIT

In the urban rail system, passengers board at origin stations to enter the network, then move dynamically between sections, and finally get off at destination stations to leave the network. Passengers spend most of their travel time on sections, and the root cause of urban rail passenger congestion lies in the insufficient capacity of sections, which in turn leads

to passengers gathering at stations. Thus, to facilitate the modeling, it is necessary to master the dynamic movement process of passengers in sections of the urban rail network. We define a spatio-temporal propagation coefficient of passenger flow, denoted by $Q^f_{r,d}\left(\tau^0,\tau\right)$. $Q^f_{r,d}\left(\tau^0,\tau\right)$ represents the probability that passengers who depart from direction f of rail station r during period τ^0 pass through section d at period τ ($\tau^0 \le \tau$), it is related to the composition of passengers' travel OD at origin stations, the travel paths of passengers, and the passing rate of paths to section, briefly, it can be calculated as Eq. (18).

$$Q^f_{r,d}\left(\tau^0,\tau\right) = \sum_{s\in \mathrm{S},(r,s)\in f}\left[b_{rs}\left(\tau^0\right)\times\sum_{u\in U^f_{rs}}\left(q^u_{rs}\left(\tau^0\right)\times p^u_d\left(\tau^0,\tau\right)\right)\right], \quad \forall r\in S,\forall d\in D,\forall f\in F,\forall\tau\in T,\tau^0\le\tau \tag{18}$$

where $b_{rs}\left(\tau^0\right)$ is the selection ratio of terminal station s, specifically, the ratio that newly arriving passengers in rail station r during period τ^0 toward for station s, which is the quotient of $P_{rs}\left(\tau^0\right)$ and $P^f_r\left(\tau^0\right)$; $q^u_{rs}\left(\tau^0\right)$ is the selection proportion of path u, specifically, the proportion that passengers of OD (r,s) during period τ^0 select path u, and we adopt a Logit model to calculate it; $p^u_d\left(\tau^0,\tau\right)$ is the passing rate of path u to section d, specifically, it is the probability that passengers who depart in period τ^0 with path u pass through section d at PFC period τ, it can be estimated from the running time of sections on path u; U^f_{rs} is the set of effective paths for OD (r,s) in direction f.

Once the spatio-temporal propagation coefficient of passenger flow is predetermined, the passenger throughput of each section during each period can be extrapolated.

B. OBJECTIVE FUNCTIONS

The integrated optimization of BRA with PFC for urban rail transit aims to reduce the average additional travel time for all affected passengers. Meanwhile, urban rail operators hope more retained passengers wait for the upcoming trains to guarantee their interests. Therefore, we consider two objectives in optimizing the combined strategies of urban rail PFC and BRA, detailed as below.

1) OBJECTIVE FUNCTION 1: MINIMIZE THE AVERAGE ADDITIONAL TRAVEL TIME OF AFFECTED PASSENGERS

As the number of affected passengers varies with the different combined strategies of PFC and BRA, we measure the benefit of all affected passengers by their average additional travel time.

$$\mathrm{Min}\ z_1 = \frac{T^{add}_s + T^{add}_t + T^{add}_b}{P_{pc} + P_{ba}} \tag{19}$$

where T^{add}_s, T^{add}_t and T^{add}_b have been detailed in Section IV; P_{pc} and P_{ba} are the numbers of passengers affected by urban rail PFC and BRA, respectively. The methods of calculating them will be detailed below.

In the first PFC period, the number of passengers affected by PFC is exactly the controlled passenger volume. In the subsequent periods, as the retained passengers must be satisfied at first according to the principle of FCFS (first-come-first-service), if the inbound passenger volume in a period is less than the retained passenger volume of the previous periods, all newly arriving passengers of this period are affected; otherwise, only the controlled passengers are affected. Hence, P_{pc} can be calculated as Eq. (20).

$$P_{pc} = \sum_{\tau\in T}\sum_{r\in\tilde{S}}\sum_{f\in F}\left(P^f_r(\tau) - max\left\{0, X^f_r(\tau) - S^f_r(\tau-1)\right\}\right) \tag{20}$$

P_{ba} can be calculated by summing the affected passenger volume of all bus ODs, shown below.

$$P_{ba} = \sum_{(v,w)} P(v,w) \tag{21}$$

2) OBJECTIVE FUNCTION 2: MAXIMIZE THE OPERATING REVENUE OF URBAN RAIL TRANSIT

$$\max z_2 = \sum_{\tau\in T}\sum_{r\in\tilde{S}}\sum_{f\in F}\left(X_{rs}(\tau)\times m^{urt}_{rs}\right) \tag{22}$$

where m^{urt}_{rs} is the urban rail fare for OD (r,s), $X_{rs}(\tau)$ is inbound passenger volume of OD (r,s) during PFC period τ, which can be calculated as follows.

$$X_{rs}(\tau) = \left(1-\mu^f_r(\tau)\right)\times\left[P_{rs}(\tau) + S_{rs}(\tau-1)\right], \quad \forall\tau\in T,\forall r\in\tilde{S},\forall s\in \mathrm{S},\forall(r,s)\in f \tag{23}$$

C. CONSTRAINTS

1) CONSTRAINTS OF PFC FOR URBAN RAIL TRANSIT

(1) Passenger demand constraints

For any PFC station, its inbound passenger volume in up and down directions during each PFC period must not exceed its passenger demand volume, and should be non-negative.

$$0 \le X^f_r(\tau) \le P^f_r(\tau) + S^f_r(\tau-1), \forall\tau\in T,\forall r\in\tilde{S},\forall f\in F \tag{24}$$

(2) Passing capacity constraints of entry gates

This constraint ensures that all permitted inbound passengers can smoothly pass through the entry gates at PFC stations. For any station, its sum of the inbound passenger volume in up and down directions during each period should not be greater than its passing capacity of all entry gates.

$$\sum_{f\in F} X^f_r(\tau) \le G_r, \quad \forall\tau\in T,\ \forall r\in\tilde{S} \tag{25}$$

(3) Constraints of transport capacity in rail sections

The passengers traveling in any rail section during each period should not exceed its transport capacity, shown

as Eq. (26).

$$\sum_{r\in S}\sum_{f\epsilon F}\sum_{\tau^0=1}^{\tau}\left[X_r^f\left(\tau^0\right)\times Q_{r,d}^f\left(\tau^0,\tau\right)\right] \le R_d\left(\tau\right),\forall\tau\in T,\forall d\in\bar{D} \quad (26)$$

The left part of the less-than-equal sign in Eq. (26) is the passenger throughput of rail section d during PFC period τ.

(4) Passing capacity constraints in transfer channels

This constraint ensures that the passenger volume assigned to any transfer channel during each PFC period does not exceed its maximum capacity.

If transfer channel d is unidirectional, its pass capacity constraint is shown as Eq. (27).

$$\sum_{r\in S}\sum_{f\epsilon F}\sum_{\tau^0=1}^{\tau}\left(X_r^f\left(\tau^0\right)\times Q_{r,d}^f\left(\tau^0,\tau\right)\right)\le UTC_d, \quad \forall\tau\in T,\forall d\in D\backslash\bar{D} \quad (27)$$

For a bidirectional transfer channel, its passengers in both directions should be uniformly constrained. Thus, the transfer channel passing capacity constraint for each bidirectional transfer channels is shown as Eq. (28).

$$\sum_{r\in S}\sum_{f\epsilon F}\sum_{\tau^0=1}^{\tau}\left(X_r^f\left(\tau^0\right)\times\left(Q_{r,d}^f\left(\tau^0,\tau\right)+Q_{r,d'}^f\left(\tau^0,\tau\right)\right)\right) \le BTC_{d-d'},\forall\tau\in T,\forall d,d'\in D\bar{D} \quad (28)$$

where transfer channels d' and d are opposite in the index of origin and terminal station.

With the same length and width, the passing capacity of a bidirectional channel is often smaller than that of a unidirectional one due to the interference of opposite passengers.

(5) Platform capacity constraints

As the capacity of a platform area is limited, the total number of passengers waiting on a platform should not exceed its capacity. There are only inbound passengers waiting on platforms in non-transfer stations, while in transfer stations, there are both inbound and transfer passengers. Note that outbound passengers of PFC stations are assumed to not occupy platform capacity according to assumption (1), the platform capacity constraint can be shown as follows.

$$\sum_{f\in F}X_r^f\left(\tau\right)+TI_r\left(\tau\right)\le P_r\times\frac{\sum_{f\in F}h_r^f\left(\tau\right)}{2},\forall\tau\in T,\forall r\in S \quad (29)$$

where $TI_r\left(\tau\right)$ denotes the number of passengers transferred into station r during period τ, and it can be calculated as Eq. (30).

$$TI_r\left(\tau\right)=\sum_{d\in D\backslash\bar{D}}\left[\beta_{d,r}\times\sum_{k\in S}\sum_{f\epsilon F}\sum_{\tau^0=1}^{\tau}\left(X_k^f\left(\tau^0\right)\times Q_{k,d}^f\left(\tau^0,\tau\right)\right)\right],\forall\tau\in T,\forall r\in S \quad (30)$$

where $\beta_{d,r}$ is a binary parameter, when station r is the terminal of section d, $\beta_{d,r}=1$; otherwise, $\beta_{d,r}=0$.

- *Constraints of BRA*

(1) Value constraints of BRA decision variables

The value of decision variable Y_l^r can be either 0 or 1.

$$Y_l^r=\begin{cases}1 & \text{If bus route } l \text{ is adjusted to } \bar{l}_r\\ 0 & \text{Otherwise}\end{cases},\forall r\in\tilde{S},\forall l\in L_r \quad (31)$$

(2) Constraints that each bus route is allowed to be adjusted once at most

For a candidate adjustable bus route, at most one of its adjustment schemes can be executed during peak hours.

$$\sum_{r\in\tilde{S}}Y_l^r\le 1,\quad \forall l\in L_r \quad (32)$$

(3) Maximum number constraints of adjustable bus routes

The BRA will not only affect the travel of some original bus passengers, but also bring difficulties in operation and management. It is not appropriate to adjust too many bus routes during peak hours.

$$\sum_{l\in L_r}Y_l^r\le n_{max} \quad (33)$$

(4) Stopping capacity constraints of bus stations

A long queue of vehicles at a bus station will reduce road capacity and affect the efficiency of bus operations. To prevent the bus fleet from lining up, the number of stopping routes at any bus station should not exceed its stopping capacity, detailed as follows.

$$m_v^0+\sum_{r\in\tilde{S}}\sum_{l\in L_r}\left[Y_l^r\times\varepsilon\left(\bar{l}_r,v\right)\right]\le m_v^{max},\quad \forall v\in V \quad (34)$$

where $\varepsilon\left(\bar{l}_r,v\right)$ is a ternary parameter, it indicates the relationship among bus station v, original bus route l and its corresponding adjustment scheme $\bar{l}_r$, if bus route $\bar{l}_r$ stops at bus station v and bus route l does not stop at bus station v, $\varepsilon\left(\bar{l}_r,v\right)=1$; if route l stops at station v and route $\bar{l}_r$ does not stop at station v, $\varepsilon\left(\bar{l}_r,v\right)=-1$; otherwise, $\varepsilon\left(\bar{l}_r,v\right)=0$.

2) CONSISTENCY CONSTRAINT BETWEEN PFC AND BRA

If a PFC station controls no passengers during the whole peak hours, there is no need to adjust any bus route to serve the controlled passengers there; otherwise, some bus routes can be adjusted for these passengers. Hence, the consistency constraint between PFC and BRA is given as follows.

$$0\le\sum_{l\in L_r}Y_l^r\le|L_r|\times\sum_{\tau\in T}\sum_{f\in F}C_r^f\left(\tau\right),\quad \forall r\in\tilde{S} \quad (35)$$

where $|L_r|$ is the number of candidate adjustable bus routes for PFC station r. Specifically, if station r controls no passengers, i.e., $\sum_{\tau\in T}\sum_{f\in F}C_r^f\left(\tau\right)=0$, there is no need to adjust any bus route for station r, $\sum_{l\in L_r}Y_l^r=0$. Conversely, if station r controls some passengers, i.e., $\sum_{\tau\in T}\sum_{f\in F}C_r^f\left(\tau\right)>0$, some bus routes can be adjusted for station r, and it is also feasible to not adjust any bus route, i.e., $\sum_{l\in L_r}Y_l^r\ge 0$.

VI. SOLUTION ALGORITHM

The above model contains two objectives, numerous decision variables and constraints. It is a constrained bi-objective optimization problem, and difficult to solve via exact algorithms. This section designs a multi-objective particle swarm optimization based on dual-population co-evolution (DPCMOPSO) to solve it.

DPCMOPSO is an extension and improvement of particle swarm optimization (PSO) [30]. Initially, PSO is just designed to solve single-objective problems. In 2004, Coello *et al.* [31] combined PSO with Pareto dominance, proposed a multi-objective particle swarm optimization (MOPSO), and they introduced an external archive to store non-inferior solutions during the evolution.

To solve our proposed model via DPCMOPSO, this paper firstly relaxes some constraints and generates some feasible solutions as an initial particle swarm. Based on these initial particles, an iterative optimization is performed by updating their velocity and position. During the evolution, a hybrid constraint processing method based on dual-population co-evolution and repairing infeasible solutions is designed to deal with constraints. Meanwhile, a dynamic distributed method based on crowding distance is adopted to maintain the external archive.

A. INITIAL SOLUTION GENERATION

As PSO is a population-based evolutionary algorithm, we need to generate a set of initial solutions for the first evolution. Our proposed model contains PFC variables and BRA variables, and BRA variables is oriented to PFC variables. Hence, we first generate PFC variables based on PFC constraints, then generate BRA variables according to consistency constraints and BRA constraints.

In our proposed model, many constraints are related to multi-dimensional variables, and it is difficult to limit the value range of a single variable, such as PFC constraints (24), (26)–(29), and consistency constraint (35). To generate initial feasible solutions, we design an initial solution generation strategy based on relaxing constraints. Firstly, we relax some constraints to better limit the value range of variables; then utilize the relaxed constraints to generate initial solutions; finally, we check the feasibility of the generated solutions and eliminate the infeasible solutions.

Obviously, for a PFC station, the retained passenger volume is no greater than the controlled passenger volume, i.e., $S_r^f(\tau) \le C_r^f(\tau)$, and the controlled passenger volume during a PFC period is not greater than the difference between the cumulative arriving passenger volume and the cumulative inbound passenger volume, i.e., $C_r^f(\tau) \le \sum_1^\tau P_r^f(\tau) - \sum_1^\tau X_r^f(\tau)$. As $S_r^f(\tau) \le C_r^f(\tau) \le \sum_1^\tau P_r^f(\tau) - \sum_1^\tau X_r^f(\tau)$ is satisfied, constraints (24) and (35) can be relaxed as follows.

$$0 \le \sum_1^\tau X_r^f(\tau) \le \sum_1^\tau P_r^f(\tau), \quad \forall \tau \in T, \quad \forall r \in \tilde{S}, \forall f \in F \tag{36}$$

$$\sum_{l \in L_r} Y_l^r \le |L_r| \times \sum_{\tau \in T} \sum_{f \in F} \left(\sum_1^\tau P_r^f(\tau) - \sum_1^\tau X_r^f(\tau) \right), \quad \forall r \in \tilde{S} \tag{37}$$

Moreover, due to the non-negativity of the transferred passenger volume $TI_r(\tau)$, we can relax the constraint (29) as follows.

$$\sum_{f \in F} X_r^f(\tau) \le P_r \times \frac{\sum_{f \in F} h_r^f(\tau)}{2}, \quad \forall \tau \in T, \ \forall r \in S \tag{38}$$

After relaxing the above constraints, we can generate a set of initial feasible solutions as shown in Algorithm 1.

Algorithm 1 The Generation of Initial Solutions

Step 1: Set the initial solution index $n = 0$, the initial population $IP = \emptyset$, the size of initial population N_p;

Step 2: Based on constraints (25), (36) and (38), randomly generate a set of $X_r^f(\tau), \forall \tau \in T, \forall r \in \tilde{S}, \forall f \in F$;

Step 3: Check whether all $X_r^f(\tau)$ satisfy constraints (26)-(29), if true, go to Step 4; otherwise, return to Step 2;

Step 4: According to the value of $X_r^f(\tau)$, randomly generate a set of $Y_l^r, \forall r \in \tilde{S}, \forall l \in L_r$ that satisfy constraints (31)-(33) and (37). $X_r^f(\tau)$ and Y_l^r form a complete set of solutions $S^{I,n}$;

Step 5: Check whether all Y_l^r satisfy constraint (34), if true, go to Step 6; otherwise, return to Step 2;

Step 6: Calculate the controlled passenger volumes and conduct passenger flow assignment in the order of PFC periods, and adjust $X_r^f(\tau+1)$ after the passenger flow assignment of period τ to satisfy constraint (24);

Step 7: Check whether all Y_l^r and $C_r^f(\tau)$ satisfy constraint (35), if true, let $n = n + 1$, insert $S^{I,n}$ into IP, and go to Step 8; otherwise, return to Step 2;

Step 8: Compare n with N, if $n \ge N$, output IP and stop iteration; otherwise, return to Step 2 and continue to generate new initial solutions.

B. A HYBRID CONSTRAINT PROCESSING METHOD

PSO is a random search algorithm, it lacks a clear constraint processing method, and can only solve unconstrained optimization problems. To deal with the constraints in our model and ensure the convergence speed of the algorithm, we propose a hybrid constraint processing method based on dual-population co-evolution [32] and repairing infeasible solutions.

During the optimization, we divide particles into feasible and infeasible particles according to whether they meet all constraints. Accordingly, we set two populations, one is feasible population, and the other is infeasible population. The particles in the feasible population evolve in the objective space, constantly looking for the optimal Pareto frontier, and the particles in the infeasible population are optimized with the goal of minimizing constraint violations.

By expressing the constraints with the inequality and equality forms, i.e., $g_j(x) \le 0$ and $h_j(x) = 0$, the constraint

violation degree of a particle can be calculated as follows.

$$G_j(\vec{x}) = \begin{cases} \max\{0, g_j(\vec{x})\} & 1 \le j \le p \\ \max\{0, |h_j(\vec{x})| - \delta\} & p+1 \le j \le q \end{cases} \quad (39)$$

$$G(\vec{x}) = \sum_{j=1}^{q} G_j(\vec{x}) \quad (40)$$

where q is the total number of constraints; p is the number of inequality constraints; δ is the tolerance level for equality constraints; $g_j(\vec{x})$ and $h_j(\vec{x})$ are the value of particle $\vec{x}$ in inequality constraint g_j and equality constraint h_j, respectively; $G_j(\vec{x})$ is the violation degree of particle $\vec{x}$ to constraint j, and $G(\vec{x})$ is the total constraint violation degree of particle $\vec{x}$. The smaller $G(\vec{x})$ is, the closer particle $\vec{x}$ is to the feasible region. If $G(\vec{x}) = 0$, it indicates that particle $\vec{x}$ meets all constraints and it is a feasible particle, otherwise, particle $\vec{x}$ is an infeasible particle.

The dual-population co-evolution strategy can guide the infeasible solutions to evolve in a feasible direction by optimizing their constraint violation degrees. However, the evolution of PSO is random and prone to produce numerous infeasible solutions which may cause the algorithm hard to converge. Hence, we also adopt an infeasible solution repairing strategy to reduce the proportion of infeasible solutions, which is shown in Algorithm 2. For each infeasible particle, we first try to repair them with tractable constraints. If repairing successfully, add them into the feasible population; otherwise, put them into the infeasible population.

Through this hybrid constraint processing strategy, we cannot only increase the proportion of feasible particles but also extract information from the evolution process of the infeasible particles, so that the global search ability of the algorithm can be improved.

Algorithm 2 The Repairing of an Infeasible Particle

Step 1: Check whether all $X_r^f(\tau)$ of the particle are non-negative, if true, go to Step 2; otherwise, set the negative $X_r^f(\tau)$ to 0 and go to Step 2;

Step 2: Check whether all $X_r^f(\tau)$ of the particle satisfy constraints (25) and (38), if true, go to Step 3; otherwise, pull $X_r^f(\tau)$ back to the boundary and go to Step 3;

Step 3: Check whether all $X_r^f(\tau)$ and Y_l^r of the particle satisfy constraint (37), if true, go to Step 4; otherwise, adjust the value of Y_l^r and go to Step 4;

Step 4: Check whether all Y_l^r of the particle satisfy constraint (32), if true, go to Step 5; otherwise, for $\sum_{r\in\tilde{S}} Y_l^r > 1, l \in L_r$, randomly pick one Y_l^r from $Y_l^r = 1, r \in \tilde{S}$ to take the value of 1, and others take 0, make $\sum_{r\in\tilde{S}} Y_l^r \le 1, \forall l \in L_r$ established, go to Step 5;

Step 5: Check whether all Y_l^r of the particle satisfy constraint (33), if true, go to Step 6; otherwise, randomly pick $n_{max} Y_l^r$ from $Y_l^r = 1, l \in L_r$ to take 1, all others take 0, make $\sum_{l\in L_r} Y_l^r \le n_{max}$ established, go to Step 6;

Step 6: Calculate the controlled passenger volume of the particle and conduct passenger flow assignment in the order of PFC periods, and adjust $X_r^f(\tau+1)$ after the passenger flow assignment of period τ to satisfy constraint (24);

Step 7: Check whether all $X_r^f(\tau)$, $C_r^f(\tau)$ and Y_l^r of the particle satisfy the constraints (26)-(29), (34) and (35), if true, the repair is successful, and the particle is classified into the feasible population; otherwise, the particle is classified into the infeasible population.

C. PATICLES' UPDATING

1) PARTICLES' VELOCITY AND POSITION UPDATING

The velocity and position of each particle in PSO are expressed as a vector, whose dimension depends on the number of decision variables. We use N and M to denote the size of the population and the number of decision variables respectively. The velocity and position vector of the particle i, denoted by $\boldsymbol{X}_i$ and $\boldsymbol{V}_i$, can be characterized as follows.

$$\boldsymbol{V}_i = (v_{i1}, v_{i2}, \cdots, v_{iM}), i = 1, 2, \cdots, N \quad (41)$$

$$\begin{aligned} \boldsymbol{X}_i = (x_{i1}, x_{i2}, \cdots, x_{iM}) = \Big(& \left[X_1^1(1)\right]_i, \\ & \left[X_1^2(1)\right]_i, \cdots, \left[X_r^f(\tau)\right]_i, \cdots, \left(Y_1^1\right)_i, \\ & \left(Y_2^1\right)_i, \cdots, \left(Y_l^r\right)_i, \cdots \Big), \\ & i = 1, 2, \cdots, N \end{aligned} \quad (42)$$

The particles' velocity and position updating are the random search process of the algorithm. The particles' velocity is composed of inertia, personal cognition and social cognition three parts, and it updates as Eq. (43).

$$v_{ij}^{(t+1)} = w \cdot v_{ij}^t + c_1 r_1 \left[pbest_{ij}^t - x_{ij}^t\right] + c_2 r_2 \left[gbest_{ij}^t - x_{ij}^t\right], \quad i = 1, 2, \cdots, N;\ j = 1, 2, \cdots, M \quad (43)$$

where t is the number of iterations, w is the inertial parameter; c_1 and c_2 are personal and social learning factors respectively; $pbest_{ij}^t$ and $gbest_{ij}^t$ denote the personal and global best position of variable j in particle i after t iterations. In MOPSO, the selection of personal best position ($pbest$) and global best position ($gbest$) is very crucial, we will introduce them in detail later.

As PFC and BRA variables are integer and binary variables respectively, their position updating equations are different, which are shown in Eq. (44) and Eq. (45) respectively.

$$x_{ia}^{(t+1)} = round\left[x_{ia}^t + v_{ia}^{(t+1)}\right], \quad i = 1, 2, \cdots, N;\ a = 1, 2, \cdots, M_1 \quad (44)$$

$$x_{ib}^{(t+1)} = \begin{cases} 1 & r < \frac{1}{1+\exp\left(-v_{ib}^{(t+1)}\right)} \\ 0 & \text{otherwise} \end{cases}, \quad i = 1, 2, \cdots, N;\ b = 1, 2, \cdots, M_2 \quad (45)$$

In Eq. (44), round[ ] represents the rounding function; M_1 is the number of PFC variables, $M_1 = 2 \times \left|\tilde{S}\right| \times |T|$, in which

$\left|\tilde{S}\right|$ and $|T|$ are the number of PFC stations and periods respectively. In Eq. (45), r is a random number in the range [0, 1]; M_2 is the number of BRA variables, $M_2 = \sum_{r\in\tilde{S}} |L_r|$, in which $|L_r|$ is the number of bus routes in L_r.

2) SELECTION OF PBEST AND GBEST

The *pbest* and *gbest* of all particles need to be determined before updating their velocity, the *pbest* refers to the best position that a particle has explored during the evolution, reflecting the particle's memory of its own experience; the *gbest* refers to the best position explored by all particles during the evolution, reflecting the cooperation between particles. In single-objective optimization, the quality of a particle can be directly judged by the objective function. Nevertheless, this paper focuses on a bi-objective optimization, and it is hard to compare the quality of all particles through the objective function as there are multiple non-inferior solutions. Hence, we design some criteria to select the *pbest* and *gbest*.

In the first iteration ($t = 1$), the initial position of a particle is regarded as its *pbest*. In the later iterations ($t \geq 2$), the *pbest* of particle i after t iteration, denoted by $pbest_i^t$, can be selected as follows.

(1) If the position of particle i after t iterations, denoted by x_i^t, is infeasible, $pbest_i^t = pbest_i^{t-1}$;

(2) If x_i^t is feasible, compare the dominance of x_i^t with $pbest_i^{t-1}$ in terms of two objectives. When $pbest_i^{t-1}$ is superior to x_i^t in both two objectives, or superior to x_i^t in one and equal to x_i^t in the other, it can be inferred that $pbest_i^{t-1}$ dominates x_i^t, $pbest_i^t = pbest_i^{t-1}$; otherwise, $pbest_i^t = x_i^t$.

This paper adopts a dual-population co-evolution strategy, and the selection of the *gbest* for particles in the feasible and infeasible populations is different.

For the feasible population, we design a priority-based selection method in three levels to select the *gbest* for each particle from the external archive. Before implementing this method, we need to calculate the crowding distance of all particles in the external archive and the gravity distance of the current particles to all particles in the external archive.

For a particle in the external archive, its crowding distance depends on its adjacent particles, which can calculated as follows.

$$C_d^k = \frac{|z_1(x_{k+1}) - z_1(x_{k-1})|}{z_1^{max} - z_1^{min}} + \frac{|z_2(x_{k+1}) - z_2(x_{k-1})|}{z_2^{max} - z_2^{min}} \tag{46}$$

where C_d^k is the crowding distance of particle k in the external archive; x_{k+1} and x_{k-1} are the positions of two adjacent particles of particle k, respectively; $z_1(x)$ and $z_2(x)$ represent the two objectives of x respectively; z_1^{max} and z_1^{min} are the maximum and minimum average additional travel time in the external archive, similarly; z_2^{max} and z_2^{min} are the maximum and minimum operating revenue in the external archive. In addition, the crowding distance of two extreme particles, i.e., the first and the last particles in the external archive, is infinite.

The gravity distance between particle i and particle k, denoted by $G_d^{i,k}$, can calculated as Eq. (47).

$$G_d^{i,k} = \sqrt{\left(\frac{|z_1(x_i^t) - z_1(x_k)|}{\gamma\left(z_1^{max} - z_1^{min}\right)}\right)^2 + \left(\frac{|z_2(x_i^t) - z_2(x_k)|}{\gamma\left(z_2^{max} - z_2^{min}\right)}\right)^2} \tag{47}$$

where γ ranges from 0.1 to 0.2. If the gravity distance between x_i^t and x_k is smaller than the gravity radius, it indicates that particle k is within the gravity radius of particle i, and the position of particle k is taken as the candidate *gbest* of particle i. The gravity radius is related to the number of objective functions, the value of the gravity radius is $\sqrt{2}$ in this paper.

The priority-based selection method in three levels places the extreme particles in the external archive at the first priority, the closest Pareto particles at the second priority, and the particles with the largest crowding distance at the third priority, the *gbest* of particle i after each iteration can be selected as follows.

(1) If an extreme optimal particle is within the gravity radius of particle i, taking this particle as the *gbest* of particle i;

(2) When (1) is not satisfied, finding out the particle with the smallest gravity distance to particle i from the external archive, and comparing this distance with the gravity radius. If this distance is smaller, taking this particle as the *gbest* of particle i;

(3) When neither (1) nor (2) is satisfied, taking the particle with the largest crowding distance in the external archive as the *gbest* of particle i.

In the feasible population, each particle has a *gbest*, while in the infeasible population, all particles share a *gbest*. After each evolution, we calculate the constraint violation degree of all infeasible particles, and select the particle with the smallest constraint violation degree as the *gbest* of all particles in the infeasible population.

3) UPDATING AND MAINTENANCE OF EXTERNAL ARCHIVE

In MOPSO, the external archive is to store the non-dominated solution. In our algorithm, the *gbest* of particles in the feasible population is selected from the external archive. The final external archive is the set of optimal solutions, also called as Pareto frontier. Hence, the external archive is crucial, and it is necessary to update and maintain it during the evolution.

To update the external archive, we should add the non-dominated particles in the feasible population into it after each iteration and delete its dominated particles.

The number of non-dominated solutions increases during the evolution so that it exceeds the limited size of the external archive. To maintain the size limit of the external archive, we adopt a dynamic distributed method based on crowding distance [33]. Specifically, when the number of non-dominated solutions exceeds the size of the external archive, we first calculate the crowding distance of all non-dominated solutions, then find out the solution with the

smallest crowding distance, and finally delete it. By repeating the above steps, we can delete these dense solutions in the external archive to ensure the diversity of the external archive and the Pareto frontier.

D. STEPS OF DPCMOPSO

To summarize, the specific steps of the DPCMOPSO are shown as Algorithm 3.

Algorithm 3 The Steps of the DPCMOPSO

Step 1: Initialize evolution parameters (w, c_1, c_2), the size of population N_p, the size of external archive N_E; set two termination conditions: the maximum iterations T_{max} and the maximum consecutive iterations TC_{max};

Step 2: Set the number of iterations $t = 0$, generate N_p initial feasible particles according to Algorithm 1, and initialize the velocity of all particles;

Step 3: Calculate z_1 and z_2 for all initial particles, find out non-dominated solutions and add them into the external archive to build an initial external archive, and set the number of initial consecutive iterations $t' = 1$;

Step 4: Select the *pbest* and *gbest* for all particles;

Step 5: Update the velocity and position of all particles, and set $t = t + 1$;

Step 6: Judge the feasibility of all particles, and classify the feasible particles into the feasible population; invoke Algorithm 2 to repair the infeasible particles and divide them into corresponding populations;

Step 7: Calculate z_1 and z_2 for all particles in the feasible population, update and maintain the external archive;

Step 8: Check whether the external archive is updated, if true, go to Step 9, otherwise, set $t' = t' + 1$, go to Step 9;

Step 9: Calculate the constraint violation degree of all particles in the infeasible population;

Step 10: Judge whether $t \geq T_{max}$ and $t' \geq TC_{max}$ are satisfied. If any of them is true, terminate the algorithm and output the current external archive as the Pareto frontier, otherwise, go to Step 4.

VII. NUMERICAL EXPERIMENTS

In this section, an urban rail network and a bus network are constructed, based on them, a series of comparative experiments are implemented to demonstrate the feasibility of the proposed model and the DPCMOPSO. The DPCMOPSO is coded in MATLAB, and run on a PC computer with 3.7 GHz Intel ® Xeon® CPU, 128G memory and Windows 10 operating system.

A. NETWORK CONSTRUCTION AND PARAMETER SETTINGS

As shown in Fig. 5, we construct a regional urban rail network with 5 lines and 21 stations, as well as a bus network with 57 stations. Among the 21 rail stations, there are 13 non-transfer stations and 8 transfer stations. Non-transfer and transfer stations are represented by colored hollow dots and black dashed boxes, respectively. We have mentioned in section II that each transfer station is defined as multiple different stations. Thus in Fig. 5, each transfer station contains multiple different stations, and the 21 rail stations are regarded as 30 stations. Moreover, we set all 30 stations as PFC stations.

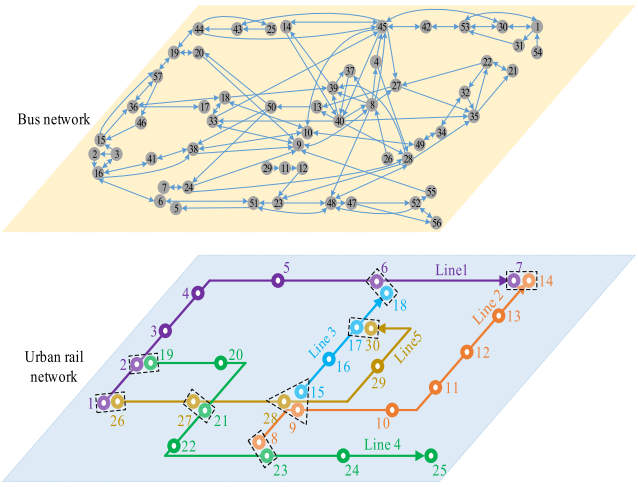

FIGURE 5. Regional urban rail network and bus network.

The urban rail network contains 70 sections, including 50 rail sections and 20 transfer channels. Among the 20 transfer channels, there are 4 pairs of bidirectional transfer channels and 12 unidirectional channels. As the constructed urban rail network is a regional network, numerous passengers from the external network also occupy the section capacity of this regional network. For simplification, the section capacity given in this paper is the residual capacity after considering the occupancy of external passengers. In all experiments, the peak hours are set from 7 a.m. to 9 a.m. and are discretized into 8 PFC periods with equal length of 15 minutes. During each PFC period, the number of trains arriving in each direction of each rail station is set to 5.

The passing capacity of all entry gates during a PFC period and the platform capacity of 30 stations are shown in Table 3. The passing capacity of the transfer channels during a period is shown in Table 4. The transport capacity of the 50 rail sections during each period is shown in Appendix. The newly arriving passenger volume in two directions at 30 rail stations during each period is also shown in Appendix.

Fig. 5 also shows the bus network, including the locations of 57 bus stations and the traffic conditions between stations before the BRA. The bus network contains 35 bus routes, of which routes 1 to 15 are fixed bus routes, and routes 16 to 35 are candidate adjustable routes. 20 candidate adjustable routes can be adjusted to bus stations near 14 PFC stations, and constitute 55 bus adjustment schemes. It is noteworthy that several stations divided by a rail transfer station are equivalent here, and they are not repeated when considering the bus adjustment schemes. 35 original bus routes and 55 bus adjustment schemes are both shown in Appendix.

TABLE 3. The passing capacity of entry gates and the platform capacity.

Station	1	2	3	4	5	6	7	8	9	10	11	12	13	14	15
G_r (person/period)	1200	1200	1200	1800	1500	1800	1200	1800	1200	1500	2250	2250	1500	2250	1500
P_r (person)	360	360	360	360	360	540	360	600	600	600	600	600	600	600	600
Station	16	17	18	19	20	21	22	23	24	25	26	27	28	29	30
G_r (person/period)	1500	1500	2250	2250	1500	1800	1800	1800	1500	2250	800	1500	1500	2250	1500
P_r (person)	600	600	750	535	535	535	535	535	535	535	875	700	700	700	700

TABLE 4. The passing capacity of transfer channels.

Bidirectional													
Transfer channel	1→26, 26→1			7→14, 14→7			8→23, 23→8			9→15, 15→9			
$BTC_{d-d'}$ (person/period)	750			1250			1500			1000			
Unidirectional													
Transfer channel	2→19	6→18	17→30	21→27	9→28	15→28	19→2	18→6	30→17	27→21	28→9	28→15	
UTC_d (person/period)	635	625	625	938	938	625	625	625	625	938	938	635	

For convenience, we first regard the 35 original bus routes and 55 bus adjustment schemes as a virtual bus network, and search all feasible paths for each rail OD and affected bus OD in the virtual network. After that, we record the required bus routes for each path and sort them by generalized costs in ascending order in advance, so that we can determine the effective paths according to available bus routes promptly.

The values of the DPCMOPSO parameters in the experiments are shown in Table 5.

TABLE 5. The values of the DPCMOPSO parameters in the experiments.

Parameters	Notations	Values
Inertial parameter	w	0.4~0.9
Individual learning factor	c_1	1.5
Social learning factor	c_2	1.5
Size of population	N_p	200
Size of external archive	N_E	20
Maximum iterations	T_{max}	500
Maximum consecutive iterations	TC_{max}	50

B. PERFORMANCE OF INTEGRATED OPTIMIZATION OF BRA WITH PFC

To demonstrate the performance of the proposed model and DPCMOPSO, an experiment is implemented in the constructed network. We set n_{max} as 10, and invoke the DPCMOPSO to solve the integrated optimization problem of BRA with PFC (hereinafter abbreviated PFCBRA). The computation time is 18627 seconds.

Fig. 6 shows the average of the two objective functions in the external archive with iterations. The average additional travel time and operating revenue of the initial external archive are the highest and the lowest, respectively, indicating that the quality of initial solutions is poor. The optimization efficiency of the two objective functions is very high at first and gradually flattens out. During the evolution, due to the addition of new extreme solutions to the external archive, the average additional travel time occasionally increases, and the operating revenue sometimes declines. However, it is conducive to improving the diversity of the Pareto frontier. On the whole, the average additional travel time and the

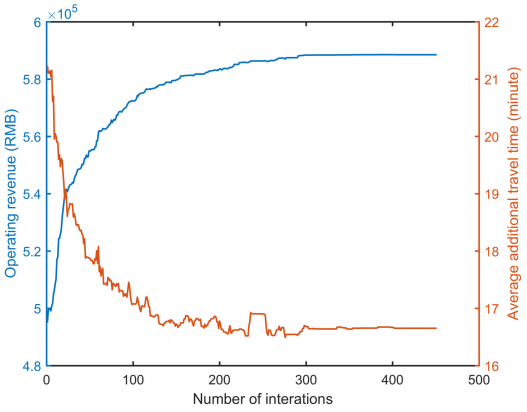

FIGURE 6. The average of the two objective functions in the external archive with iterations.

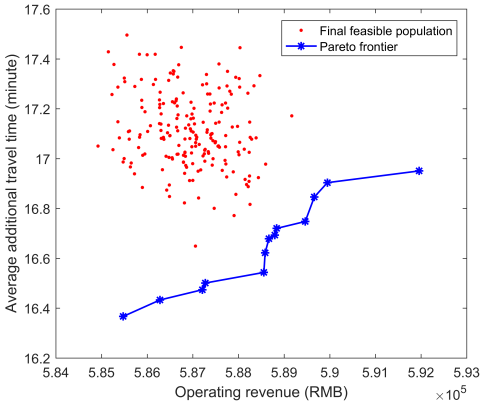

FIGURE 7. The pareto frontier and the final feasible population in the PFCBRA.

TABLE 6. 11 indicators of 13 optimal solutions in the PFCBRA.

Solution number	z_1(minute)	z_2(RMB)	n_{ba}	P_{total}	P_{ba}	P_{pc}	P_s	P_t	$\bar{T}_s^{add}$(min)	$\bar{T}_t^{add}$(min)	$\bar{T}_b^{add}$(min)
1	16.37	585473	10	220866	17675	203191	161321	41870	20.22	7.93	1.19
2	16.43	586281	10	222053	17205	204848	163575	41273	20.20	7.53	2.02
3	16.47	587209	10	220467	16631	203836	163069	40767	20.24	7.68	1.15
4	16.50	587274	10	225565	18410	207155	167855	39300	20.23	7.53	1.67
5	16.54	588557	10	222475	17679	204796	164738	40058	20.30	8.10	0.64
6	16.62	588584	10	222702	16936	205766	166420	39346	20.25	7.74	1.60
7	16.68	588668	10	226523	18167	208356	170333	38023	20.21	7.87	1.99
8	16.69	588796	10	223872	18187	205685	166465	39220	20.49	7.99	0.72
9	16.72	588835	10	223713	18073	205640	166094	39546	20.53	8.27	0.20
10	16.75	589463	10	221301	16091	205210	166275	38935	20.24	7.99	1.82
11	16.85	589661	10	223793	16138	207655	169192	38463	20.36	8.08	0.91
12	16.90	589948	10	222951	15524	207427	169552	37875	20.31	7.95	1.49
13	16.95	591958	10	222130	16470	205660	168295	37365	20.40	8.07	1.86
Average	**16.65**	**588516**	**10**	**222955**	**17168**	**205787**	**166399**	**39388**	**20.31**	**7.90**	**1.33**

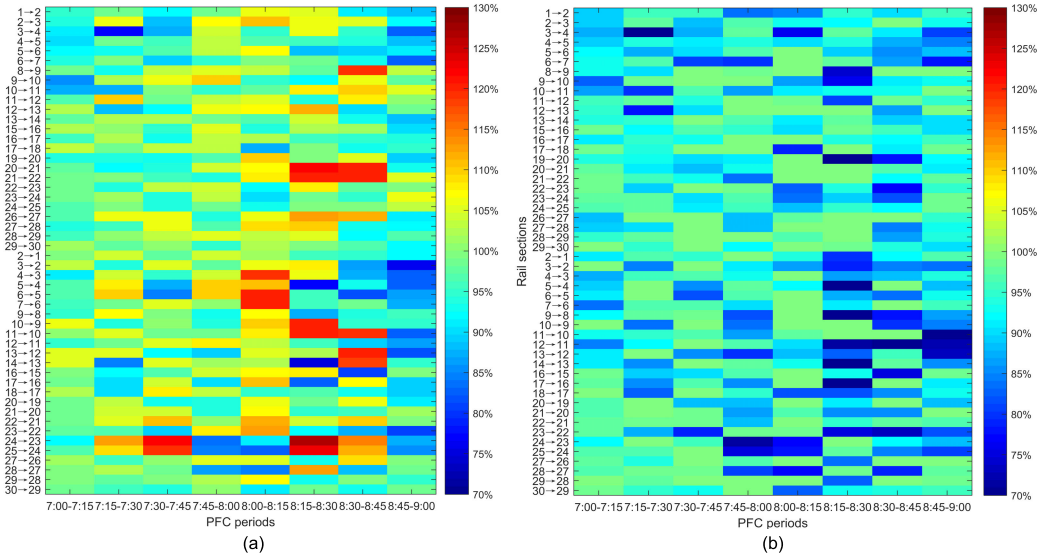

FIGURE 8. The ratio of passenger demand to transport capacity. (a) Before the integrated optimization. (b) After the integrated optimization.

operating revenue are declining and increasing, respectively, and they remain unchanged at last. Thus it can be inferred that we have obtained the optimal Pareto frontier of the PFCBRA, and the DPCMOPSO has a good convergence.

The Pareto frontier and the final feasible population in the PFCBRA are shown in blue and red respectively in Fig. 7. The Pareto frontier contains 13 optimal solutions, the operating revenue is from 585473 to 591958 RMB, and the average additional travel time is from 16.37 to 16.95 minutes. We find that as the operating revenue increases, the average additional travel time also increases. It can be inferred that with the integrated strategy of BRA with PFC, the average additional travel time increases with the inbound passenger volume, and it takes more time to travel by urban rail transit than by bus when the urban rail network is congested.

In Table 6, 11 indicators of 13 optimal solutions in the PFCBRA are given. Specifically, z_1 and z_2 are two objectives respectively; n_{ba} is the total number of adjusted bus routes; P_{total} is the number of all affected passengers; P_{ba} and P_{pc} are the numbers of passengers affected by BRA and urban rail PFC, respectively; P_s and P_t are the total retained and shifted passenger volumes; $\bar{T}_s^{add}$, $\bar{T}_t^{add}$ and $\bar{T}_b^{add}$ are the average additional travel time for retained, shifted and affected original bus passengers respectively. In all solutions, the average additional travel time of all retained and shifted passengers are about 20 and 8 minutes, respectively. The average additional travel time of shifted passengers is significantly less than that of retained passengers, demonstrating that shifting behavior can save a lot of travel time than retention. Meanwhile, we find that the average additional travel time of affected original bus passengers is from 0.20 to 2.02 minutes, which indicates that BRA only results in a slight increase in the travel time for original bus passengers. In addition, the average number of passengers affected by

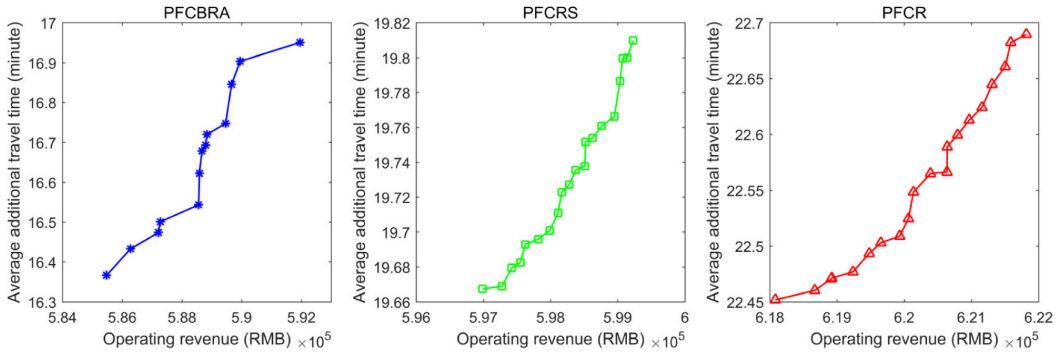

FIGURE 9. The final pareto frontier in the PFCBRA, PFCRS and PFCR.

TABLE 7. The transport capacity of rail sections.

Rail sections	PFC periods								Rail sections	PFC periods							
	1	2	3	4	5	6	7	8		1	2	3	4	5	6	7	8
1→2	501	750	1189	1177	1045	983	1472	1334	2→1	684	989	937	724	1010	1290	1179	1059
2→3	526	635	1811	1147	1231	1295	1161	1419	3→2	479	1688	1149	1707	1504	1405	2185	2214
3→4	605	1842	1634	1038	1749	1114	1456	1694	4→3	788	896	1382	1327	802	1328	2018	1866
4→5	836	942	1200	1001	1294	1336	1259	1308	5→4	645	961	2031	1269	1296	2736	1800	1938
5→6	674	1189	1230	919	825	1560	1511	1135	6→5	607	943	2229	1111	734	1755	2343	1894
6→7	564	826	1460	1378	1317	1614	1562	1706	7→6	739	1021	913	1160	486	1309	1152	1579
8→9	612	1780	1191	1731	2040	2885	1137	1886	9→8	744	1171	1819	2607	2268	4177	3473	2834
9→10	1512	1341	1378	1691	3237	3620	2396	2388	10→9	146	2433	1726	2583	2372	1853	3336	3121
10→11	1573	2457	1835	2354	2530	1998	1715	1699	11→10	787	1578	1856	2448	2583	1981	1742	4282
11→12	1295	1076	1675	1611	1893	2904	1823	1838	12→11	1344	2036	1319	1715	2973	3746	4114	4050
12→13	985	2971	2368	1634	1878	1330	2710	1691	13→12	1060	1708	2366	3144	2878	3175	1991	4526
13→14	699	1180	1014	1484	1993	1168	1855	1870	14→13	1301	2774	1145	1889	2423	4541	1666	2864
15→16	435	1266	1883	1255	2279	1960	1743	1889	16→15	842	2060	1998	1477	1599	1632	3346	1271
16→17	829	934	1591	1020	958	1695	1581	1068	17→16	925	2078	1356	2534	1252	3359	1261	1901
17→18	405	1665	1291	1211	2592	1832	1993	1310	18→17	1357	2656	1582	1995	2785	2638	2509	2242
19→20	1238	1505	1763	2243	1836	3110	2231	2445	20→19	404	715	1555	1634	962	1572	826	1513
20→21	919	1809	1794	1817	2134	1348	1121	2272	21→20	450	896	1022	1959	1323	2333	1935	1116
21→22	433	1269	2225	3333	2733	2180	1733	1920	22→21	667	1010	845	1933	1451	2011	1252	1495
22→23	381	1483	1341	2165	3152	2303	2772	1899	23→22	669	1562	2547	1708	1627	3311	3282	3084
23→24	261	703	1788	1730	3097	2513	2572	1262	24→23	1746	1125	1036	4175	3778	1516	1878	3275
24→25	254	396	1112	1057	1921	1528	1415	784	25→24	1459	1173	903	3556	3743	1275	1549	3164
26→27	2181	1639	1583	2974	2131	1959	1538	2908	27→26	508	2201	1736	1887	2022	3326	1347	1335
27→28	1728	2325	1553	2787	2132	2252	3501	3045	28→27	734	1620	2393	3825	4115	1795	3457	1655
28→29	798	965	837	879	1649	1440	2529	1701	29→28	716	1653	1454	1393	1134	2421	1180	1277
29→30	215	980	675	1273	653	772	1068	1357	30→29	732	1457	1402	913	1946	1189	1436	741

BRA in 13 optimal solutions is 17168, while the average shifted passenger volume is 39388, the shifted passenger volume exceeds twice the affected passenger volume. Therefore, it can be concluded that taking BRA measures can effectively save travel time for controlled passengers, and its advantages outweigh its disadvantages.

Fig. 8 shows the ratio of passenger demand to transport capacity in 50 rail sections before and after the integrated optimization (taking solution 7 as an example). Before the integrated optimization, no measures are taken, the average ratio of passenger demand to transport capacity of 50 rail sections is 99.10%, however, the ratio in many rail sections exceeds 100%, and some even exceeds 120%, the contradiction between passenger demand and transport capacity is prominent. After the integrated optimization, PFC and BRA measures are adopted, the ratio of demand to capacity in each rail section, also known as the load factor, is not greater than 100%, and the average load factor of 50 rail sections is 92.13%. Hence, it can be concluded that our integrated optimization can effectively alleviate passenger congestion on the basis of making good use of transport capacity.

C. THE BENEFITS OF INTEGRATED OPTIMIZATION OF BRA WITH PFC

To further demonstrate the benefits of the integrated optimization of BRA with PFC (PFCBRA), we set two groups of comparative optimization experiments with independent PFC, one is that passengers voluntarily choose to retain and shift (hereinafter abbreviated PFCRS), the other assumes that all passengers choose to retain (hereinafter abbreviated PFCR). After removing the BRA decision variables and constraints (31)-(35), the DPCMOPSO can solve the PFCRS and

TABLE 8. The newly arriving passenger volume at rail stations.

Stations	Up direction								Stations	Down direction							
	PFC periods									PFC periods							
	1	2	3	4	5	6	7	8		1	2	3	4	5	6	7	8
1	383	753	745	963	968	1041	717	624	1	0	0	0	0	0	0	0	0
2	254	338	400	517	380	397	246	230	2	653	422	215	315	270	303	158	116
3	205	276	281	368	345	443	278	269	3	842	712	688	587	512	683	491	436
4	858	935	806	1113	702	872	588	530	4	550	583	627	779	746	635	444	368
5	426	462	697	620	636	683	558	267	5	480	618	642	921	853	721	462	317
6	530	639	598	870	911	1292	748	589	6	565	694	621	708	548	815	478	490
7	0	0	0	0	0	0	0	0	7	751	547	774	860	840	803	799	828
8	760	1051	810	1355	1451	1892	1424	1534	8	0	0	0	0	0	0	0	0
9	446	478	308	621	612	524	341	339	9	411	268	257	401	274	412	350	297
10	962	768	669	771	681	782	673	889	10	557	707	560	706	892	661	765	543
11	1339	1197	580	1052	1223	1122	1069	776	11	977	942	806	1214	1292	1078	814	919
12	1037	1144	948	1558	1322	1121	942	881	12	498	539	725	1110	1119	1103	831	688
13	169	198	118	297	264	173	123	86	13	745	694	789	1130	1369	1242	914	872
14	0	0	0	0	0	0	0	0	14	2509	1327	1443	2163	2592	2782	3061	2266
15	1259	1121	908	1189	1075	1115	589	462	15	0	0	0	0	0	0	0	0
16	592	376	310	593	407	735	361	333	16	842	620	682	667	826	889	560	376
17	862	562	716	577	819	821	742	416	17	729	284	383	511	588	526	412	363
18	0	0	0	0	0	0	0	0	18	2158	1899	2032	2302	2410	2615	1827	1515
19	1348	923	997	1797	2346	2768	2025	1527	19	0	0	0	0	0	0	0	0
20	413	572	630	1006	903	726	542	512	20	288	334	223	468	333	323	262	166
21	318	504	767	1474	1191	1128	661	540	21	323	563	302	616	551	446	310	221
22	412	645	812	964	957	904	551	499	22	428	703	467	610	721	615	392	317
23	217	204	276	522	637	700	493	360	23	260	467	477	758	899	1125	785	491
24	85	156	133	177	145	181	112	67	24	782	862	1017	1093	1057	1096	719	534
25	0	0	0	0	0	0	0	0	25	1561	1935	2349	2544	2566	2994	2268	2181
26	2384	2175	1962	2625	2961	3509	2589	2129	26	0	0	0	0	0	0	0	0
27	396	412	575	586	666	612	414	393	27	714	779	612	825	724	741	351	221
28	102	193	281	414	938	346	530	281	28	394	350	451	687	571	593	450	270
29	354	408	800	798	824	695	588	631	29	543	980	1147	1285	1518	1202	762	577
30	0	0	0	0	0	0	0	0	30	772	933	731	822	1076	904	659	356

TABLE 9. Original bus routes.

Fixed routes		Candidate adjustable routes	
Number of route	Stopping bus stations	Number of route	Stopping bus stations
1	36→18→39→37	16	52→55→9→33→18→36
2	2→16→6→51→48→47→52→56	17	21→22→27→13→50→20→19→57
3	14→45→42→53→30	18	15→57→19→44→45→42→53→30→1
4	25→43→44→19→57→36→18	19	26→8→4→45→30→1
5	3→15→36→17	20	31→53→42→45→27→13→50→24→7
6	37→40→33→18→36	21	37→40→13→50→38→41→16→3
7	30→45→40→39→37	22	14→40→28→48→47
8	3→16→41→38→10→49→34	23	37→40→35→21
9	21→22→32→34→49→10→18→36	24	56→52→48→51→6→16→3→2
10	29→11→12→23→48→47→56	25	57→19→20→9→8→27→35→22→21
11	54→1→30→53→42→45→14	26	1→30→53→42→45→43→44→19→57→46→15
12	18→36→57→19→44→25	27	7→24→9→8→45→42→53→1→31
13	34→49→10→38→41→16→3	28	3→16→38→9→8→37
14	36→18→10→49→34→32→35→22→21	29	37→40→8→48→47
15	36→18→33→9→8→37	30	36→18→33→45→30→1
		31	7→24→28→35→21
		32	1→30→45→10→49→34
		33	7→24→9→8→39→37
		34	48→28→39→14
		35	4→28→23→51→5

the PFCR. The Pareto frontier of the PFCBRA, the PFCRS and the PFCR are compared in Fig. 9.

In the PFCRS, the operating revenue is from 596987 to 599230 RMB, and the average additional travel time is from 19.67 to 19.81 minutes. In the PFCR, the two objectives are from 618081 to 621817 RMB and 22.45 to 22.69 minutes. We find that the PFCBRA can effectively shorten passengers' average additional travel time, it can save about 3 minutes

TABLE 10. Bus adjustment schemes.

Number of bus adjustment schemes	Original bus route	PFC stations	Stopping bus stations
1	16	10	52→55→28→9→33→18→36
2	16	8/23	52→55→23→9→33→18→36
3	16	24	52→55→47→9→33→18→36
4	17	12	21→22→35→27→13→50→20→19→57
5	17	17/30	21→37→13→50→20→19→57
6	17	29	21→22→27→8→13→50→20→19→57
7	17	20	21→22→27→13→18→57
8	17	2/19	21→22→27→13→36→57
9	18	2/19	15→46→57→19→44→45→42→53→30→1
10	18	5	15→57→19→44→14→45→42→53→30→1
11	19	11	26→34→8→4→45→30→1
12	19	17/30	26→8→37→4→45→30→1
13	19	16	26→8→39→4→45→30→1
14	20	17/30	31→53→42→45→37→13→50→24→7
15	20	9/15/28	31→53→42→45→27→13→50→11→24→7
16	21	9/15/28	37→40→13→50→9→38→41→16→3
17	21	2/19	37→40→13→46→16→3
18	21	20	37→40→13→18→16→3
19	22	6/18	14→45→40→28→48→47
20	22	17/30	14→37→40→28→48→47
21	22	29	14→40→8→28→48→47
22	22	9/15/28	14→40→9→28→48→47
23	22	8/23	14→40→51→48→47
24	23	29	37→40→8→35→21
25	24	9/15/28	56→52→48→51→11→16→3→2
26	25	20	57→18→9→8→27→35→22→21
27	25	16	57→19→20→13→8→27→35→22→21
28	25	17/30	57→19→20→37→8→27→35→22→21
29	25	10	57→19→20→9→49→35→22→21
30	25	11	57→19→20→9→8→34→35→22→21
31	26	5	1→30→53→42→45→14→43→44→19→57→46→15
32	27	21/27	7→24→38→9→8→45→42→53→1→31
33	27	16	7→24→9→39→45→42→53→1→31
34	27	17/30	7→24→9→37→45→42→53→1→31
35	28	16	3→16→38→9→39→37
36	29	10	37→40→8→49→48→47
37	29	9/15/28	37→40→9→48→47
38	29	8/23	37→40→23→48→47
39	30	5	36→18→33→14→45→30→1
40	30	16	36→18→33→39→45→30→1
41	30	17/30	36→18→33→37→45→30→1
42	31	9/15/28	7→24→9→28→35→21
43	31	8/23	7→24→51→28→35→21
44	31	24	7→24→47→28→35→21
45	31	11	7→24→28→34→35→21
46	32	17/30	1→30→45→37→10→49→34
47	32	16	1→30→45→40→10→49→34
48	33	8/23	7→24→51→9→8→39→37
49	33	21/27	7→24→38→9→8→39→37
50	34	8/23	48→23→39→14
51	34	9/15/28	48→10→39→14
52	34	29	48→28→8→39→14
53	34	17/30	48→28→39→37→14
54	34	6/18	48→28→39→45→14
55	35	29	4→8→28→23→51→5

compared to the PFCRS, and 6 minutes compared to the PFCR. Meanwhile, as more passengers retain at rail stations and they will occupy these rail sections with surplus capacity in the subsequent periods, the operating revenue in the PFCR and PFCRS is a bit higher. In general, compared with the PFCR, the operating revenue in the PFCBRA has dropped by about 5%, while the average additional travel time has dropped by about 25%; compared with the PFCRS, the operating revenue in the PFCBRA has dropped by about 2%, while the average additional travel time has dropped by about 15%. Besides, in the PFCBRA, the total additional travel time of all passengers is from 3612843 to 3778124 minutes; in the PFCRS, it is from 4346638 to 4377826 minutes, while in the PFCR, it is from 5199735 to 5269815 minutes, thus the total time saved in the PFCBRA is evident.

In summary, the integrated optimization of BRA with PFC can greatly reduce the travel time for passengers at the expense of a small amount of urban rail operating revenue.

VIII. CONCLUSION AND FUTURE STUDIES

To relieve passenger congestion in the urban rail network, PFC is a common method in megacities during peak hours. To facilitate the travel of controlled passengers at rail stations, this paper proposes a BRA strategy, and studies an integrated optimization problem of BRA with PFC for urban rail transit. The shift or retention choices for controlled passengers, as well as the additional travel time for retained, shifted and original bus passengers with the integrated strategy are analyzed. To characterize the integrated problem mathematically, an integer non-linear programming model is proposed with two objectives of minimizing the average additional travel time for all affected passengers and maximizing the operating revenue of urban rail transit. Since the proposed model is non-linear and contains two objectives, the DPCMOPSO is designed to solve the model, in which a hybrid constraint processing method based on feasible and infeasible population concurrent evolution, as well as repairing infeasible solutions are devised to deal with the constraints. Finally, three sets of experiments are implemented to demonstrate the performance of the integrated optimization of BRA with PFC. The experimental results show that the integrated optimization could greatly shorten passengers' travel time compared with the independent optimization of PFC.

Future studies will mainly focus on the following aspects:

(1) This paper only considers static passenger demand in the urban rail network. In reality, passenger demand is always dynamic or random. Thus, research based on dynamic or random passenger demand can be accounted for in our future research.

(2) For better dealing with real large-scale instances, a more effective algorithm should be further studied.

IX. APPENDIX

The transport capacity of rail sections is shown in Table 7, in which PFC period 1 represents 7:00 a.m.-7:15 a.m., PFC period 2 represents 7:15 a.m.-7:30 a.m., and so on, PFC period 8 represents 8:45 a.m.-9:00 a.m.. The newly arriving passenger volume at rail stations is shown in Table 8.

The stopping bus stations of 35 original bus routes are shown in Table 9. 55 bus adjustment schemes are illustrated in Table 10, in which the corresponding original bus routes, PFC stations, and stopping bus stations are given.

REFERENCES

[1] Z. Jiang, W. Fan, W. Liu, B. Zhu, and J. Gu, "Reinforcement learning approach for coordinated passenger inflow control of urban rail transit in peak hours," *Transp. Res. C, Emerg. Technol.*, vol. 88, pp. 1–16, Mar. 2018.

[2] H. Niu and X. Zhou, "Optimizing urban rail timetable under time-dependent demand and oversaturated conditions," *Transp. Res. C, Emerg. Technol.*, vol. 36, pp. 212–230, Nov. 2013.

[3] E. Hassannayebi, A. Sajedinejad, and S. Mardani, "Urban rail transit planning using a two-stage simulation-based optimization approach," *Simul. Model. Pract. Theory*, vol. 49, pp. 151–166, Dec. 2014.

[4] Y. Gao, L. Kroon, M. Schmidt, and L. Yang, "Rescheduling a metro line in an over-crowded situation after disruptions," *Transp. Res. B, Methodol.*, vol. 93, pp. 425–449, Nov. 2016.

[5] T. Zhang, D. Li, and Y. Qiao, "Comprehensive optimization of urban rail transit timetable by minimizing total travel times under time-dependent passenger demand and congested conditions," *Appl. Math. Model.*, vol. 58, pp. 421–446, Jun. 2018.

[6] S. Wang, W. Zhang, and X. Qu, "Trial-and-error train fare design scheme for addressing boarding/alighting congestion at CBD stations," *Transp. Res. B, Methodol.*, vol. 118, pp. 318–335, Dec. 2018.

[7] H. Yang and Y. Tang, "Managing rail transit peak-hour congestion with a fare-reward scheme," *Transp. Res. B, Methodol.*, vol. 110, pp. 122–136, Apr. 2018.

[8] X.-Y. Xu, J. Liu, H.-Y. Li, and M. Jiang, "Capacity-oriented passenger flow control under uncertain demand: Algorithm development and real-world case study," *Transp. Res. E, Logistics Transp. Rev.*, vol. 87, pp. 130–148, Mar. 2016.

[9] W. Li and J. Zhou, "The optimize management of passenger organization in transfer station based on dynamic passenger flow analysis," *Procedia-Social Behav. Sci.*, vol. 96, pp. 1322–1328, Nov. 2013.

[10] X.-Y. Xu, J. Liu, H.-Y. Li, and J.-Q. Hu, "Analysis of subway station capacity with the use of queueing theory," *Transp. Res. C, Emerg. Technol.*, vol. 38, pp. 28–43, Jan. 2014.

[11] Q. Zhang, B. Han, and D. Li, "Modeling and simulation of passenger alighting and boarding movement in Beijing metro stations," *Transp. Res. C, Emerg. Technol.*, vol. 16, no. 5, pp. 635–649, Oct. 2008.

[12] S. Baee, F. Eshghi, S. M. Hashemi, and R. Moienfar, "Passenger boarding/alighting management in urban rail transportation," in *Proc. Joint Rail Conf.*, Apr. 2012, pp. 823–829.

[13] S. Seriani and R. Fernandez, "Pedestrian traffic management of boarding and alighting in metro stations," *Transp. Res. C, Emerg. Technol.*, vol. 53, pp. 76–92, Apr. 2015.

[14] L. Wang, X. Yan, and Y. Wang, "Modeling and optimization of collaborative passenger control in urban rail stations under mass passenger flow," *Math. Problems Eng.*, vol. 2015, pp. 1–8, Dec. 2015.

[15] M. Jiang, H.-Y. Li, X.-Y. Xu, S.-P. Xu, and J.-R. Miao, "Metro passenger flow control with station-to-station cooperation based on stop-skipping and boarding limiting," *J. Central South Univ.*, vol. 24, no. 1, pp. 236–244, Feb. 2017.

[16] S. Li, M. M. Dessouky, L. Yang, and Z. Gao, "Joint optimal train regulation and passenger flow control strategy for high-frequency metro lines," *Transp. Res. B, Methodol.*, vol. 99, pp. 113–137, May 2017.

[17] J. Shi, L. Yang, J. Yang, and Z. Gao, "Service-oriented train timetabling with collaborative passenger flow control on an oversaturated metro line: An integer linear optimization approach," *Transp. Res. B, Methodol.*, vol. 110, pp. 26–59, Apr. 2018.

[18] Z. Jiang, J. Gu, W. Fan, W. Liu, and B. Zhu, "Q-learning approach to coordinated optimization of passenger inflow control with train skip-stopping on a urban rail transit line," *Comput. Ind. Eng.*, vol. 127, pp. 1131–1142, Jan. 2019.

[19] R. Liu, S. Li, and L. Yang, "Collaborative optimization for metro train scheduling and train connections combined with passenger flow control strategy," *Omega*, vol. 90, pp. 1–18, Jan. 2020.

[20] X. Xu, H. Li, J. Liu, B. Ran, and L. Qin, "Passenger flow control with multi-station coordination in subway networks: Algorithm development and real-world case study," *Transportmetrica B, Transp. Dyn.*, vol. 7, no. 1, pp. 446–472, Feb. 2018.

[21] L. Zeng, J. Liu, Y. Qin, L. Wang, and J. Yang, "A passenger flow control method for subway network based on network controllability," *Discrete Dyn. Nature Soc.*, vol. 2018, pp. 1–12, Sep. 2018.

[22] J.-J. Kong and C. Zhang, "Critical subway stations identification for passenger flow control by applying network controllability," *J. Chin. Inst. Eng.*, vol. 41, no. 6, pp. 530–537, Sep. 2018.

[23] J. Shi, L. Yang, J. Yang, F. Zhou, and Z. Gao, "Cooperative passenger flow control in an oversaturated metro network with operational risk thresholds," *Transp. Res. C, Emerg. Technol.*, vol. 107, pp. 301–336, Oct. 2019.

[24] J. Yang, J. G. Jin, J. Wu, and X. Jiang, "Optimizing passenger flow control and bus-bridging service for commuting metro lines," *Comput.-Aided Civil Infrastruct. Eng.*, vol. 32, no. 6, pp. 458–473, Apr. 2017.

[25] J. Liang, J. Y. Wu Qu, H. Yin, X. Qu, and Z. Gao, "Robust bus bridging service design under rail transit system disruption," *Transp. Res. E, Logistics Transp.*, vol. 132, pp. 97–116, Dec. 2019.

[26] J. G. Jin, L. C. Tang, L. Sun, and D.-H. Lee, "Enhancing metro network resilience via localized integration with bus services," *Transp. Res. E, Logistics Transp. Rev.*, vol. 63, pp. 17–30, Mar. 2014.
[27] J. G. Jin, K. M. Teo, and A. R. Odoni, "Optimizing bus bridging services in response to disruptions of urban transit rail networks," *Transp. Sci.*, vol. 50, no. 3, pp. 790–804, Aug. 2016.
[28] J. Guo, L. Jia, Y. Qin, and H. Zhou, "Cooperative passenger inflow control in urban mass transit network with constraint on capacity of station," *Discrete Dyn. Nature Soc.*, vol. 2015, Jan. 2015, Art. no. 695948.
[29] S. Chowdhury, A. Ceder, and B. Schwalger, "The effects of travel time and cost savings on commuters' decision to travel on public transport routes involving transfers," *J. Transp. Geography*, vol. 43, pp. 151–159, Feb. 2015.
[30] J. Kennedy and R. Eberhart, "Particle swarm optimization," in *Proc. IEEE Int. Conf. Neural Netw.*, vol. 4, Nov. 1995, pp. 1942–1948.
[31] C. A. C. Coello, G. T. Pulido, and M. S. Lechuga, "Handling multiple objectives with particle swarm optimization," *IEEE Trans. Evol. Comput.*, vol. 8, no. 3, pp. 256–279, Jun. 2004.
[32] A. Ebrahim Sorkhabi, M. Deljavan Amiri, and A. R. Khanteymoori, "Duality evolution: An efficient approach to constraint handling in multi-objective particle swarm optimization," *Soft Comput.*, vol. 21, no. 24, pp. 7251–7267, Nov. 2016.
[33] G. Peng, Y.-W. Fang, W.-S. Peng, D. Chai, and Y. Xu, "Multi-objective particle optimization algorithm based on sharing–learning and dynamic crowding distance," *Optik*, vol. 127, no. 12, pp. 5013–5020, Jun. 2016.

WENLIANG ZHOU received the Ph.D. degree in transportation engineering from Central South University, in 2010. He is currently an Associate Professor with the School of Traffic and Transportation Engineering, Central South University. His research interests include timetable optimization for rail transit, and integrated optimization of urban rail transit and bus.

PANPAN HU received the B.S. degree in transportation from the Wuhan University of Technology, China, in 2018. She is currently pursuing the M.S. degree with the School of Traffic and Transportation Engineering, Central South University, China. Her research interests include passenger flow control of urban rail transit, and integrated optimization of urban rail transit and bus.

YU HUANG received the B.S. degree in transportation from East China Jiaotong University, China, in 2019. She is currently pursuing the M.S. degree with the School of Traffic and Transportation Engineering, Central South University, China. Her research interests include train scheduling and train circulation planning.

LIANBO DENG received the Ph.D. degree in transportation engineering from Central South University, in 2007. He is currently a Professor with the School of Traffic and Transportation Engineering, Central South University. His research interests include train plan optimization for rail transit and passenger flow assignment.